Title

Using Wearable Devices and Deep Learning Methods to Predict Risk of Injury for Ergonomic Evaluation

Author

Yan, Yishu

Publication Date

2024

Using Wearable Devices and Deep Learning Methods to Predict Risk of Injury for Ergonomic Evaluation

By

Yishu Yan

A dissertation submitted in partial satisfaction of the

requirements for the degree of

Doctor of Philosophy

in

Engineering - Mechanical Engineering

in the

Graduate Division

of the

University of California, Berkeley

Committee in charge:

Professor Grace D. O'Connell, Co-Chair
Professor Carisa Harris Adamson, Co-Chair
Professor Grace X. Gu
Professor Ellen Eisen

Fall 2024

Using Wearable Devices and Deep Learning Methods to Predict Risk of Injury for Ergonomic Evaluation

Abstract

Using Wearable Devices and Deep Learning Methods to Predict Risk of Injury for Ergonomic Evaluation

by

Yishu Yan

Doctor of Philosophy in Engineering - Mechanical Engineering

University of California, Berkeley

Professor Grace D. O'Connell, Co-Chair

Professor Carisa Harris Adamson, Co-Chair

Work-related musculoskeletal disorders (WMSDs) represent a significant challenge in occupational health, with risks increasing when the physical demands of a job surpass an employee's capabilities. Accurate Physical Demands Analysis (PDA) is essential for developing job descriptions, pre-employment screening, conducting ergonomic assessments, and supporting return-to-work programs. PDAs require identifying Occupational Physical Activities (OPAs) and quantifying physical exposures.

Traditionally, OPAs have been identified through self-reports, observation and direct measurements. While effective, these methods can be less reliable, labor-intensive, and limited in dynamic work settings. Emerging technologies, such as wearable devices, provide promising alternatives by offering automated and scalable solutions. However, research applying these methods to recognize OPAs in complex work tasks remains limited. This study utilized inertial measurement units (IMUs) and deep learning techniques to identify thirteen distinct OPAs, including seven whole body and six upper body activities, both in isolation and within three simulated work tasks designed to replicate real-world conditions.

Building on OPA identification, the study focused on quantifying physical exposures critical for ergonomic evaluation, particularly in manual lifting. IMUs were used to measure lift origins and destinations, reducing intrusiveness and enabling the capture of more lifting events. These findings establish reliable methods for both quantifying OPAs and assessing physical exposures, with significant potential for improving workplace safety and reducing the risk of WMSDs.

Table of contents

Contents

List of Figures

List of Tables

Acknowledgements

First and foremost, I would like to express my sincere gratitude to my PhD advisors, Professor Grace D. O'Connell and Professor Carisa Harris Adamson. I am deeply grateful to Professor Grace D. O'Connell for her invaluable guidance, thoughtful support, and mentorship throughout my research. I want to express my heartfelt thanks to Professor Carisa Harris Adamson, from the School of Public Health, for her continuous guidance, insightful feedback, and hands-on experience in the lab. Their expertise, encouragement, and unwavering dedication have been instrumental in shaping my research and my growth as a scholar. I have been truly inspired by their attitude toward science and research, which has motivated me to approach my work with greater curiosity and determination. I have thoroughly enjoyed my research, studies, and life over the past five years, largely due to their careful guidance and support in all aspects of my academic and personal life during my PhD.

I would also like to extend my heartfelt thanks to my colleagues and lab mates for their support, camaraderie, and collaboration throughout my PhD journey. Their valuable insights, assistance, and shared experiences have made my research both more enjoyable and meaningful. I am truly grateful for the collaborative environment we fostered, which allowed me to grow as a researcher and build lasting professional relationships. I also want to thank all the research participants for their time, effort, and willingness to contribute to my study. Without their participation, this research would not have been possible. Their involvement was crucial to the success of my work, and I am deeply appreciative of their contribution. A special thanks also goes to the students I had the opportunity to instruct as a Graduate Student Instructor. Their enthusiasm, curiosity, and hard work made my teaching experience both fulfilling and rewarding.

Above all, I would like to express my deepest gratitude to my family, especially my parents, for their unwavering love, support, and encouragement throughout my PhD journey. Being far from home while studying abroad has presented many challenges, but their constant care and belief in me have kept me motivated and grounded. Despite physical distance, their love has been an unyielding source of strength. I am also incredibly grateful to my beloved fur baby, Bling, who entered my life during the COVID-19 pandemic. Her companionship has provided me with much-needed comfort and joy, helping me through the difficult moments of being away from family. I am truly fortunate to have such a loving and supportive family, both human and feline, that has made this journey possible.

1 Introduction

1.1 Work-Related Musculoskeletal Disorders

Musculoskeletal disorders affect the body's nerves, tendons, muscles, and ligaments. Workers in various industries are frequently exposed to risk factors that contribute to the development of work-related musculoskeletal disorders (WMSDs). These disorders not only impact individual workers' health but also pose substantial challenges to workplace efficiency and economic stability. According to the 2022 Workplace Safety Index, overexertion has been identified as the primary cause of disabling workplace injuries, accounting for nearly $13 billion in direct costs to businesses annually (“2022 Workplace Safety Index” 2022).

Among WMSDs, low back pain is particularly noteworthy. It is recognized as the leading cause of physical disability and productivity loss globally, underscoring its significant burden on both individuals and healthcare systems. With a lifetime prevalence of nearly 84% among adults, low back pain remains a pervasive issue, affecting workers across all sectors (“Work-Related Musculoskeletal Disorders & Ergonomics | Workplace Health Strategies by Condition | Workplace Health Promotion | CDC” 2021). WMSDs often arise from a mismatch between the physical demands of a job and the worker's physical capacity. Risk factors include repetitive motions, the application of excessive force, awkward or sustained postures, and prolonged static positions, all of which can gradually degrade musculoskeletal health over time (Odebiyi et al. 2023).

To mitigate these risks, it is essential to align physical job demands with worker capabilities through evidence-based ergonomic principles. This ensures a healthier workforce while reducing economic and productivity losses caused by WMSDs.

1.2 Physical Demand Analysis

Physical Demands Analysis (PDA) serves as a systematic procedure that quantifies and evaluates the physical requirements of a job, ensuring that job demands are appropriately matched to the workforce's capabilities. Physical demands refer to the level and duration of physical exertion generally required to perform critical tasks in support of critical job functions, such as sitting, standing, walking, lifting, carrying, reaching, pushing, and pulling (“Physical Demands” 2015). Therefore, quantifying Occupational Physical Activities (OPAs) is a key component of the PDA, providing detailed data on the workload involved in each task. This data helps identify the intensity, frequency, and duration of physical activities, which can vary depending on the job role and environment. By capturing this information, the PDA offers a comprehensive view of the physical demands needed to perform job functions.

PDA is crucial in job recruitment as it clearly defines and communicates the physical requirements of a position, providing potential candidates with a thorough understanding of the physical demands involved. This also enables employers to ensure that new hires possess the necessary physical capabilities to safely and effectively perform their job duties (Xinming et al. 2015). In job placement, PDAs are used to match workers with positions that align with their physical abilities. Properly aligning worker capabilities with job demands through PDA data helps prevent WMSDs by minimizing the risk of overexertion.

One of the most critical applications of PDA is in the Return-to-Work (RTW) process following injury/illness (Government of Canada 2024). During this process, PDA helps identify areas within different work zones where modified duties may be available. They also assist healthcare providers in understanding the specific job demands when evaluating workers' ability to return, enabling them to determine whether the worker can safely resume their pre-injury role or if modifications are necessary. This approach promotes a safe return to work, minimizing the risk of re-injury and supporting the worker's rehabilitation and reintegration into the workplace. According to the Americans with Disabilities Act (ADA), employers are required to provide accommodations to qualified individuals with disabilities to enable them to perform essential job functions safely ("The ADA: Your Responsibilities as an Employer,"). By ensuring that job demands align with the capabilities of pre-injured employees, PDA supports compliance with ADA requirements, thereby promoting an inclusive and equitable work environment.

Beyond recruitment, placement, and RTW, PDA also provides valuable information about high-risk activities that could result in elevated physical demands, warranting further evaluation using ergonomic risk assessment tools. For instance, the Revised NIOSH Lifting Equation (RNLE) can be applied to evaluate lifting activities (Ahmad and Muzammil 2023) , and the Liberty Mutual Manual Materials Handling Equations can be used to assess the risks associated with tasks such as carrying and pushing (Potvin et al. 2021). Identifying high-risk activities allows employers to prioritize targeted interventions, redesign workflows, and implement effective ergonomic solutions to reduce worker injury and enhance workplace safety.

1.3 Occupational Physical Activities

As a core component of PDA, OPAs involve specific physical activities, such as lifting, carrying, and overhead work, which can impose significant physical demands. When poorly managed, these activities increase the risk of WMSDs. Accurately quantifying OPAs is critical to align job demands with worker capacities and reduce injury risks.

Historically, various methods have been employed to measure OPAs, including self-reports, observational techniques, and direct measurements. While these approaches have provided valuable insights, they often suffer from limitations in reliability, accuracy, and efficiency (Thiese 2013; Jancey et al. 2014; Steeves et al. 2018; Melanson Jr., Freedson, and Blair 1996).

Recent advancements in technology, particularly wearable devices like inertial measurement units (IMUs) and motion-tracking systems, offer new opportunities to improve OPA quantification (Mäkela et al. 2022; J. Chen, Qiu, and Ahn 2017; Humadi et al. 2021b). These tools have the potential to enable objective, continuous, and scalable assessments, and allow for a more accurate representation of physical demands in dynamic and diverse work environments. However, challenges such as task variability and overlapping activities persist, highlighting the need for innovative solutions to enhance the precision and applicability of OPA analysis in complicated work tasks.

Given the critical role of OPAs in understanding job demands and preventing WMSDs, this research focuses on advancing OPA identification and quantification using modern technologies. By leveraging wearable devices and computational techniques, this study aims to enhance the accuracy, reliability, and scalability of OPA recognition. These advancements will contribute to more effective ergonomic risk assessments and improved physical demand analysis, ultimately supporting safer and healthier workplaces. The challenges and methodologies underlying this approach are explored in detail in Chapters 2 and 3.

1.4 Quantify Physical Exposures

Quantifying physical exposure is a critical step that follows the identification of OPAs. As discussed in Section 1.3, identifying activities such as lifting, carrying, etc. is essential for physical demand analysis. However, to comprehensively assess workplace risks, it is equally important to measure the physical exposures associated with these activities. This step provides deeper insights into the intensity, duration, and frequency of OPAs, which are closely linked to the development of WMSDs.

For example, workers performing manual material handling (MMH) tasks, such as lifting, are at heightened risk of developing WMSDs, particularly low back pain, due to repetitive movements, awkward postures, and excessive forces (Boschman et al. 2011; Coenen et al. 2014; Lu et al. 2014). Measuring exposures such as lifting frequency, hand locations is crucial to determine whether job demands are within safe limits and to design interventions that minimize injury risks. These measures are foundational to PDA.

Traditionally, ergonomic risk assessments of lifting tasks, such as those performed using the Revised NIOSH Lifting Equation (RNLE) (T. R. Waters, Putz-Anderson, and Garg 1994), rely on manually collected data for parameters like lifting frequency and hand locations. While effective, these methods are labor-intensive and prone to human error.

Recent advancements in wearable technologies, particularly inertial measurement units, offer a promising alternative for physical exposure quantification. IMUs capture position, velocity, and acceleration data, enabling continuous and objective tracking of workers' movements. This capability allows for more precise and efficient assessments, especially in dynamic and complex work tasks.

Building on the identification of OPAs, this research also focuses on leveraging IMUs to enhance the accuracy and scalability of exposure quantification. Specifically, in Chapter 4, this study details an approach for measuring key parameters of lifting tasks, such as frequency and hand locations, with promising accuracy. By integrating IMUs into ergonomic assessments, this work aims to improve PDA and contribute to safer and healthier workplaces.

1.5 Historical Context and Emerging Solutions

In January 2001, the Occupational Safety and Health Administration (OSHA) implemented an ergonomics program designed to enhance workplace safety and reduce WMSDs. This standard required the employer to establish ergonomic programs tailored to their workforce and to assess jobs for ergonomic risk factors. However, in March 2001, a resolution was signed to repeal the standard, citing concerns over the absence of a standardized and reliable approach for evaluating physical exposures and the significant costs associated with implementation ("Ergonomics Program. | OSHA.Gov | Occupational Safety and Health Administration" 2001).

Following the repeal, researchers intensified efforts to develop more robust and consistent methods for assessing ergonomic risks, particularly in MMH tasks, which are a leading cause of injuries. Despite significant progress, achieving reliable and valid risk assessments in real-world occupational settings remains challenging.

Advancements in wearable technology and machine learning offer transformative opportunities in this field. Wearable devices, integrated with sophisticated data analytics, can enable precise recognition of OPAs and provide quantitative measures of physical exposures. These innovations support evidence-based ergonomic risk assessments and hold the potential to significantly improve the identification of high-risk tasks, the design of targeted interventions, and the monitoring of ergonomic solution effectiveness.

This thesis focuses on leveraging wearable technologies and deep learning methods to advance the field of physical demand analysis. Chapters 2 and 3 explore the application of these tools in identifying OPAs, while Chapter 4 extends this work to develop reliable physical exposure assessments for manual lifting tasks.

1.6 Study Objectives

The primary objective of this research is to leverage wearable technologies and deep learning models to enhance physical demand analysis for ergonomic evaluation. Specifically, the study focuses on predicting occupational physical activities, especially during simulated tasks and developing a framework for quantifying physical exposures during manual lifting.

The sub-objectives are as follows:

- **Activity Recognition:** Use wearable devices and deep learning methods to identify occupational physical activities in simulated work tasks.
- **Physical Exposure Quantification:** Create an IMU-based system to measure key parameters such as lifting frequency and spatial distances with minimal human intervention.

In Chapter 2, a preliminary identification of OPAs using eight IMUs is introduced, showing promising results when activities were performed in isolation, along with a decline in performance during simulated work tasks. In Chapter 3, further efforts are made to recognize OPAs in a more comprehensive manner, achieving promising performance both in isolation and during simulated work tasks. In Chapter 4, the focus shifts to recognizing physical exposures, particularly during periods identified as lifting in the previous chapter, to provide the necessary information for physical demand analysis.

These efforts aim to provide a scalable, practical approach for comprehensive physical demand analysis, improving workplace safety, reducing WMSD risks, and facilitating broader adoption in diverse occupational settings.

2 Phase I: Preliminary Identification of OPAs

2.1 Introduction

Chapter 2 is based on a published paper titled "Applying wearable technology and a deep learning model to predict occupational physical activities." (Y. Yan et al. 2021)

As introduced in Chapter 1, physical demands vary significantly across different jobs, necessitating a PDA to outline the physical and environmental requirements for performing a job. The PDA includes information on the approximate duration (% of day) and magnitude (load) that different OPAs, such as lifting/lowering, carrying, kneeling, reaching, walking, and standing, take place. The PDA informs workers about the physical demands of a job before they are hired, and it provides occupational health practitioners critical information for facilitating effective return-to-work programs should an injury occur.

Various methods for quantifying OPAs include self-report, observational, and direct measurement (David 2005; Schall, Fethke, and Chen 2016). Though both self-report and observational approaches are low-cost and convenient, results can be inaccurate and unreliable, as well as time consuming (Mokhlespour Esfahani, Nussbaum, and Kong 2019). Although observational methods are the most common approach for estimating OPAs (David 2005), some have used more detailed video-based techniques to quantify the duration of OPAs with higher accuracy. Essentially, workers are recorded in real time and the video is analyzed using computer software that aggregates the amount of time spent performing different OPAs. Direct measurements of force supplement the video analysis to provide a more valid and reliable PDA; however, this approach is extremely time consuming and costly (David 2005).

Accurate and reliable quantification of OPAs required for a job description is critical for physically demanding jobs. Prospective workers rely on them to determine if they would like to pursue a job and clinicians rely on them to facilitate appropriate return-to-work plans. Further, accurate and reliable quantification of the duration, frequency and magnitude of physical demands can be useful when assessing interventions designed to reduce physical exposures associated with WMSDs. To overcome the limitations of self-report, observational, and direct measurement methods, kinematic data could be an effective approach to quantifying OPAs in the workplace. Kinematic data yield the position, velocity, and acceleration of body segments and have been used to predict the patterns and quality of movement (H. Chen et al. 2015). Conventional methods of capturing kinematic data rely principally on video analysis or an optoelectronic system to distinguish movement patterns of body segments (Song and Qu 2014b; 2014a; Harris-Adamson et al. 2015; Tammana et al. 2018). However, these laboratory methods have limitations in real work scenarios both in cost and feasibility.

Wearable technology, such as inertial measurement units (IMUs), have been used to capture human body motion for animation, optimizing athletic performance, and even optimizing patient treatment (Cuesta-Vargas, Galán-Mercant, and Williams 2010). For example, Daponte et al. (Daponte, De Vito, and Sementa 2013) developed a wireless and IMU-based system for monitoring patient motion with real-time 3D reconstruction. IMU systems have also been used by practitioners for gait and lower limb rehabilitation (Yang et al. 2019; Yeh et al. 2013). IMUs perform well when tracking the orientation of a moving object, thus, coaches and athletes use them to assess athletic performance (Groh et al., n.d.; Tessendorf et al. 2011). More recently, IMUs have been used in the workplace to quantify specific exposures that may increase the risk of injury. A smart garment using two IMU sensors was introduced by Wang et al. (Q. Wang et al. 2017) to monitor shoulder posture for treating WMSDs. Relative time series data and kinematic data from the wearable sensors (IMUs) are used to summarize the percent time spent in different physical activities and the probability of being at high risk for WMSDs (Marras 2000; Gallagher 2005). The IMU system (17 IMUs) with classification models introduced by Kim and Nussbaum (Kim and Nussbaum 2013) and Bastani, Kim, Kong, Nussbaum, and Huang (Bastani et al. 2016), classified MMH tasks for real-time applications with a higher accuracy than observational methods. These studies provide support for the use of wearable devices in predicting OPAs actively and continuously in diverse work environments, even using fewer sensors. However, the performance of using wearable devices on classifying a broader range of OPAs such as crouching, kneeling and overhead work has not been evaluated. Further, there is little, if any, work published on predicting OPAs when combined in typical simulated work tasks.

Therefore, the objective of this study was to apply deep learning models to data from eight IMUs to predict physical activities performed during simulated occupational tasks. If wearable devices can be used to predict OPAs with higher accuracy, reliability and efficiency than self-report, observational or direct methods, job descriptions and return to work programs can be standardized more effectively.

2.2 Materials and Methods

2.2.1 Study Procedure

This laboratory study collected kinematic data from 8 IMUs worn on 8 different body segments by participants who performed OPAs common in MMH jobs (Groh et al., n.d.; Marras 2000; Gallagher 2005; Bastani et al. 2016; Kelsey et al. 1984; GRANATA and MARRAS 1999; Hoogendoorn et al. 1999; Strine and Hootman 2007; Gallagher and Marras 2012; Agarwal, Steinmaus, and Harris-Adamson 2018; Harris-Adamson et al. 2016). The kinematic data were used for training a deep learning model for pattern recognition (Figure 2-1). The trained model was used to predict OPAs performed in 3 simulated work tasks. In this pilot validation study, model predictions of the OPA were validated using a frame-by-frame analysis of video collected during simulated tasks.

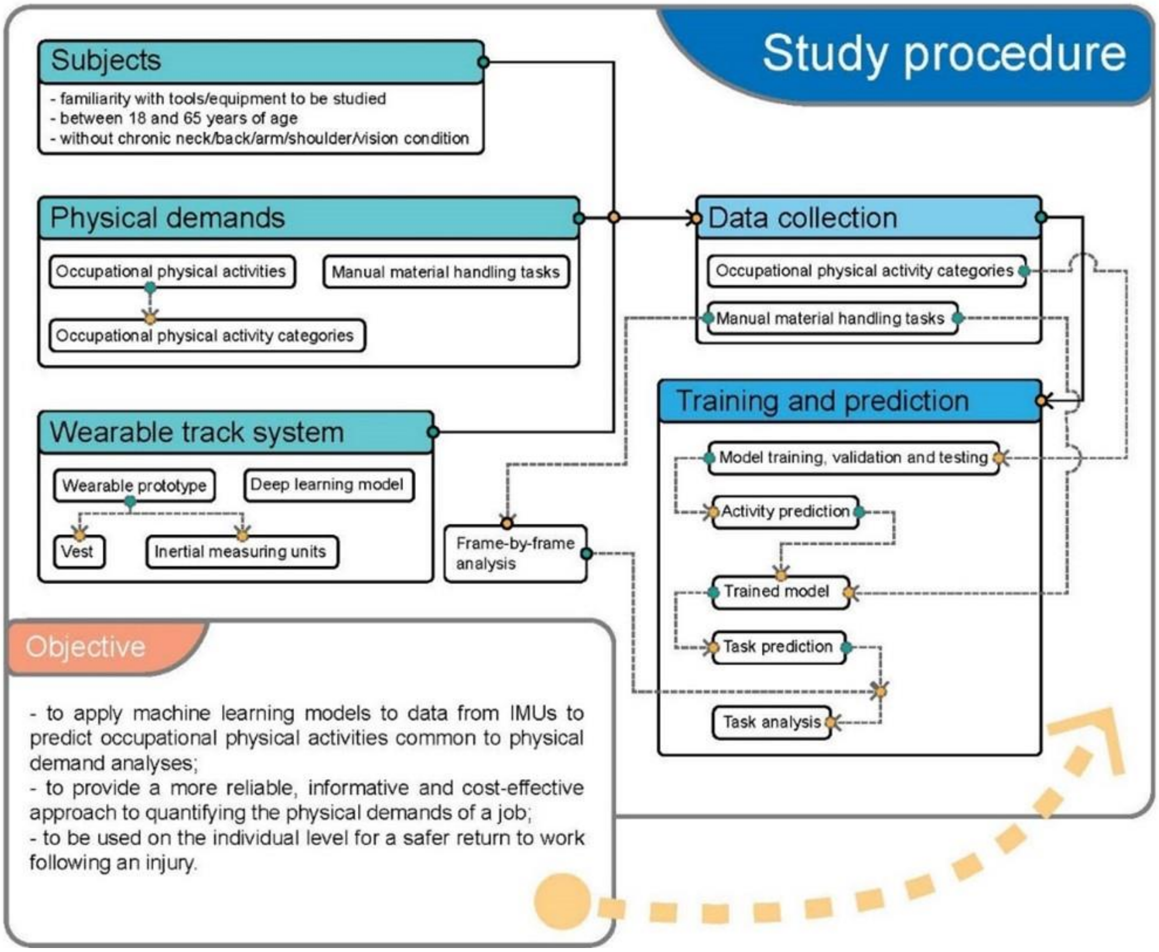

Figure 2-1 Study procedure of prediction of occupational physical activities using inertial measurement units and deep learning model

2.2.2 Participants

Subjects (*n* = 15) were recruited by email, campus, and social networks. To be included in the study, subjects needed to be between 18 and 65 years of age and willing to perform the simulated work tasks described. Subjects with neck/back/arm/shoulder/vision pain were excluded. Written informed consent was obtained from all subjects before their participation. This study was approved by the Institutional Review Board of the University of California, San Francisco (IRB# 10-04700).

2.2.3 Occupational Physical Activities and Manual Material Handling Tasks

In this study, 15 categories of occupational physical activities were selected with some OPAs performed in multiple ways to capture the variation of physical activities and prevent overfitting of the model (Table 2-1). To train the models, subjects performed activities with fixed parameters of load, duration, and repetition. Most OPAs were performed for at least 60 s each.

A subset of participants (*n* = 9) completed up to three simulated work tasks including bottle packing, carpet laying, and drilling to test the deep learning model's ability to predict OPAs while performing simulated work tasks (Figure 2-2). Except for sitting which exhibited obvious features for prediction, the bottle packing, carpet laying and drilling tasks included all OPA (Table 2-2). Verbal explanations and visual demonstrations were provided for subjects prior to performing the various OPAs and simulated work tasks. The whole procedure took approximately 2 hours per subject.

Subjects performed carpet laying and bottle packing tasks until the task was complete; all tasks were completed within 5 min. Drilling was performed for 15 s. Details for each task include:

- Bottle packing started with opening the box and putting 12 bottles into the box, which contained three rows (close, intermediate, and extended distances) and four bottles in each row. After placing the bottles in the box, the box was closed. The horizontal distances between the bottles and the body were <30 cm, 30–40 cm, and >40 cm. Next, the box was carried about two meters and placed on shelves of fixed heights ranging from floor height, waist height and shoulder height.
- The carpet laying task was performed by lifting carpet from a shelf (floor, waist and shoulder height) onto a cart. The cart was then pushed or pulled to a distance of approximately two meters. After placing the carpet on the floor, subjects were asked to lay the carpet in a pre-defined rectangle.
- The drilling task involved picking up a drill, or paint roller with one hand, walking to the designated area about two meters away and drilling overhead or on the ground. Afterwards the tool was returned to the original spot.

Table 2-1 Occupational physical activities (N of subjects = 15)

OPA Category		Activity		Load	Duration/repetition	Repetition
1	Lifting/Lowering	1	Lifting from floor to shoulder level	4.5kg (box)	15s	2
		2	Lifting from floor to waist level	4.5kg (box)	15s	2
		3	Lifting from shoulder to waist level with twist	4.5kg (box)	15s	2
		4	Lifting from shoulder to waist level without twist	4.5kg (box)	15s	2
		5	Stooped lifting from floor to waist level	4.5kg (box)	15s	2
		6	Lifting from floor to 1.5m level	4.5kg (box)	15s	2
2	One-handed lifting/lowering	7	Right-handed lifting from floor to waist level	4.5kg (box)	15s	2
		8	Left-handed lifting from floor to waist level	4.5kg (box)	15s	2
3	Pushing	9	Pushing clockwise	136kg (cart)	60s	1
		10	Pushing counterclockwise	136kg (cart)	60s	1
4	Pulling	11	Pulling clockwise	136kg (cart)	60s	1
5	One-handed pulling	12	Right-handed pulling	136kg (cart)	60s	1
		13	Left-handed pulling	136kg (cart)	60s	1
6	Standing	14	Standing	0 kg	60s	1
7	Sitting	15	Sitting	0 kg	60s	1
8	Kneeling	16	Kneeling	0 kg	60s	1
9	Static stooping	17	Static stooping	0 kg	60s	1
10	Walking	18	Walking	0 kg	60s	1
11	Crouching	19	Crouching	0 kg	60s	1
12	Crawling	20	Crawling	0 kg	60s	1
13	Carrying	21	Carrying	4.5kg (box)	60s	1
14	Reaching	22	Reaching (standing) close to body (shoulder elevation angle: 30°)	0 kg	60s	1
		23	Reaching (standing) far from body (shoulder elevation angle: 60°)	0 kg	60s	1
		24	Reaching (standing) high and far from body (shoulder elevation angle: 135°)	0 kg	60s	1
15	Overhead work	25	Static overhead work	0 kg	60s	1
		26	Dynamic overhead work	0 kg	60s	1

OPA: occupational physical activities

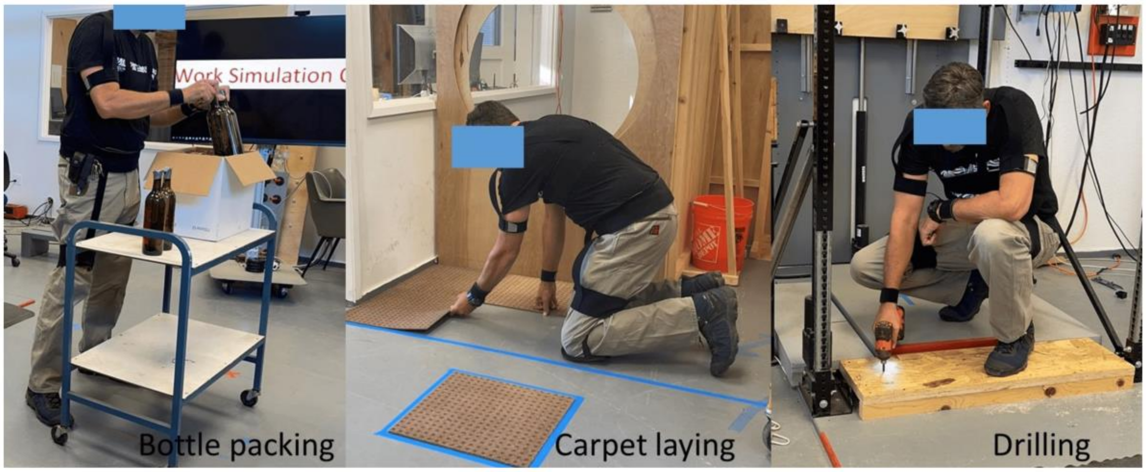

Figure 2-2 Manual material handling tasks: bottle packing, carpet laying, and drilling

Table 2-2 Manual material handling tasks (n = 9). Subjects complete MMH tasks with different handling height and OPAs covered by each task are listed

MMH task	N	Duration/repetition	OPA category covered
Bottle packing	6	Within 5 min	Standing, reaching, lifting/lowering, walking and carrying
Carpet laying	4	Within 5 min	Walking, lifting/lowering, One-handed lifting/lowering, pushing, pulling, One-handed pulling, crouching, stooping, crawling, kneeling and standing
Drilling	4	15s	Walking, lifting/lowering, carrying, stooping, overhead work and standing

2.2.4 Wearable Track Device with Inertial Measurement Units

A lightweight (<0.7 kg) prototype wearable vest and arm cuffs that housed 8 IMUs (SwiftMotion, Berkeley, CA, USA) was used to quantify the kinematics while performing OPAs (Figure 2-3). The vest was designed with a shoulder harness, belt, upper arm straps and upper leg straps made by nylon mesh fabric, which was used to fix the positions of the IMUs. The vest was available in three different sizes (small, medium, and large), and the straps were length-adjustable to allow exact positioning of the sensors, independent of the body type of the subject.

The specific positions of IMUs were as follows: (1) two were placed on the spine facing posterior, one between the 3rd and 4th thoracic spinous process (T3-T4) and the other between the 5th lumbar and 1st sacral spinous process (L5-S1); (2) two were placed on the medial segment of each upper arm facing lateral; (3) two were placed on the distal segment of each forearm just proximal to the hand facing posterior; (4) the last two were placed on the medial segment of each thigh facing posterior. With these 8 sensors and their corresponding anatomical locations it was possible to track the orientation of the trunk, upper arms, forearms, and thighs. The sensors were not placed directly on muscle bellies, as their orientation could then change during the activation of those muscles.

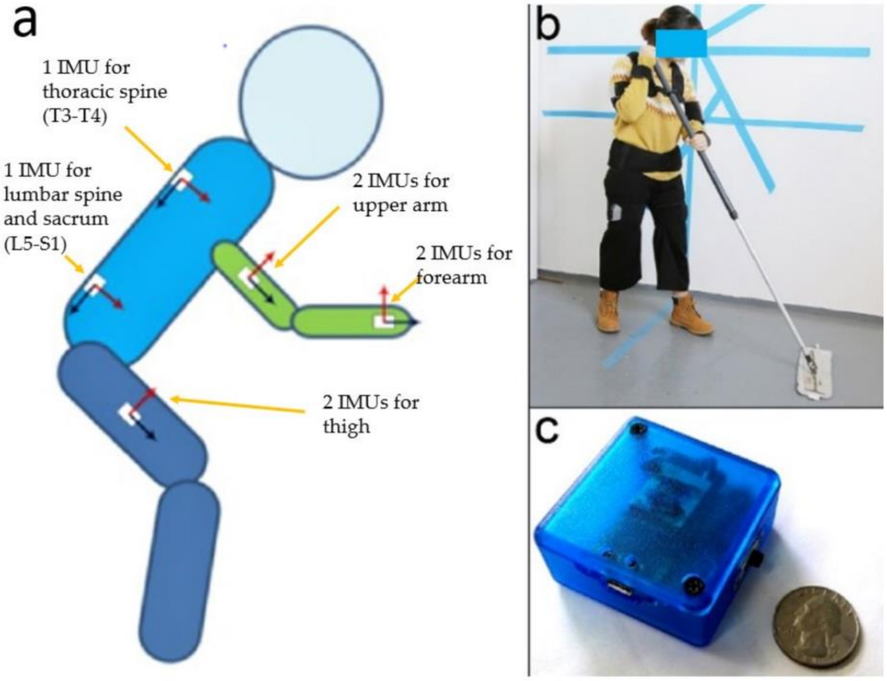

Figure 2-3 Wearable vest for occupational physical activities: (a) wearable track device and location of IMUs and their orientations (orientations were displayed as two orthogonal vectors), (b) performing manual material handling tasks with prototype, (c) IMU used in this study

The small IMUs (50 × 50 × 20 mm) developed by the researchers included three-axis accelerometers, three-axis gyroscopes, and three-axis magnetometers, which measured accelerations, velocities, and position (orientation). Data from the IMUs were recorded at a sample frequency of 10 Hz.

2.2.5 Data Collection

Time series data (1 column) and kinematic data (18 columns) were synchronized from the 8 IMUs and transmitted to a laptop by Wi-Fi dongles. The IMUs output included both the quaternion and Euler data. Kinematic data were recorded by IMU number and position (2 columns), quaternion (4 columns), Euler angle (°, 3 columns), raw acceleration (m/s2, 3 columns), linear acceleration (m/s2, 3 columns), and angular velocity (rad/s, 3 columns). The current orientation of IMUs was determined by using Euler angle following the Z-Y-Z sequence: the first rotation occurs around the Z-axis, followed by a rotation around the Y-axis and a rotation around the rotated new Z-axis. Quaternions transformed to Euler angles using Equation (2-1).

$$\mathrm{Quat2Eul}(q) = \left[\arctan\frac{2(q_0q_1+q_2q_3)}{1-2(q_1^2+q_2^2)}, \arcsin\big(2(q_0q_2-q_3q_1)\big), \arctan\frac{2(q_0q_3+q_1q_2)}{1-2(q_2^2+q_3^2)}\right]^T \qquad (2\text{-}1)$$

where, q_0 denotes the scalar part and q_1, q_2 and q_3 denote the vector part of the quaternion.

2.2.6 Model Training

The ResNet-18 structure was pre-defined, only the weights were learned during training. Error was defined as the averaged cross-entropy loss over all samples (Sangari and Sethares 2016) in one batch (Equation (2-2)). Training was not finished until the model converged (Figure 2-4a). A convolutional neural network (CNN), ResNet-18 (He et al. 2016) was used for categorical prediction. Its 18-layer implementation was robust to train the model efficiently and retain high accuracy. The time series data and kinematic data of activities based on the 15 OPA categories (Table 2-1) were converted to tensors (1 × 60 × 19) and divided into 60%, 20% and 20% for training, validation, and testing, respectively.

$$\mathrm{loss}(x, i) = \frac{1}{N}\left(-x[i] + \log\left(\sum\nolimits_j e^{x[j]}\right)\right) \qquad (2\text{-}2)$$

where, in each batch, i represented the correct OPA categories, j represented all of the OPA categories and N was the batch size. The lowest validation error across models did not necessarily identify the best model. Therefore, it was critical to save the current best model when the validation error decreased. After the training was complete, the best model was selected based on testing data accuracy (minimize empirical error). Model training and prediction were all performed using Python 2.7.

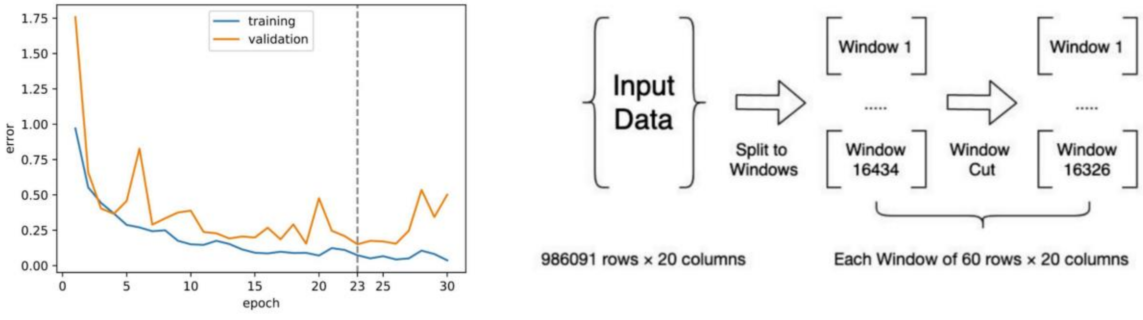

(a) (b)

Figure 2-4 Model training: (a) the training and validation error over the epoch, the model converged at epoch 23 and became overfitting afterward, (b) window cut.

The OPA categories were added to data of 15 activities as the activity's labels; the raw datasets were saved to 15 csv files. Each csv file represented one activity and was constructed in such a way that columns represented coordinates and time derivative information from one sensor and rows represented timestamps of each of the 8 sensors. Therefore, each row had 18 columns of sensor data, 1 column for the timestamp, and 1 column for the label.

The final model input data was generated by combining multiple rows together to form an image-like window. The number of rows combined (window size) was a hyperparameter of the model. The window size with the highest accuracy achieved. Each window had a size of 60 rows × 20 columns: in other words, 60 rows of sensor data, 20 columns of sensor data plus an activity label (Figure 2-4b). Finally, the overlapping window was cut. An overlapping window was defined as a window containing multiple activities and therefore it was redundant. For example, when a single window (1 s) contained both activity 1 and activity 2, this window was dropped (0.7%).

2.2.7 Task Prediction and Validation

Simulated work tasks were video-recorded at 30 frames per second and then analyzed using Multimedia Video Tasks Analysis™ (MVTA™, NexGen Ergonomics Inc., Pointe-Claire, QC, Canada). Each frame was categorized and labeled into one of the 15 OPAs (Table 2-1). Two researchers performed the task analysis using MVTA. Both researchers were trained by a senior engineer who has been using MVTA for more than 13 years. To ensure reliability and accuracy, random frames were selected by the Principal Investigator (PI), who is also one of the thesis committee members, and the senior engineer for validation. Any uncertainties in the analysis were resolved through discussions with the PI and senior engineer. Transitions (e.g., frames between standing and lifting) were allocated to the proceeding OPA.

In the occupational activity classification problems, after removing the column of activity label, each task was split into multiple 60 × 19 windows as input to the CNN. In total, 60 rows of data corresponded to roughly 1 s of “video” which was enough for a single activity to be repetitive and recognizable. The CNN analyzed these windows and mapped them to a predicted OPA. The trained CNN model was applied to the IMU data for the simulated work tasks to predict an OPA for each 1 s interval. The OPA prediction each second was compared to the results from the MVTA (Yen and Radwin 1995) to calculate model accuracy of OPA prediction (Figure 2-5). A post hoc analysis of the best three predictions of OPAs generated by the CNN model was used for further analysis.

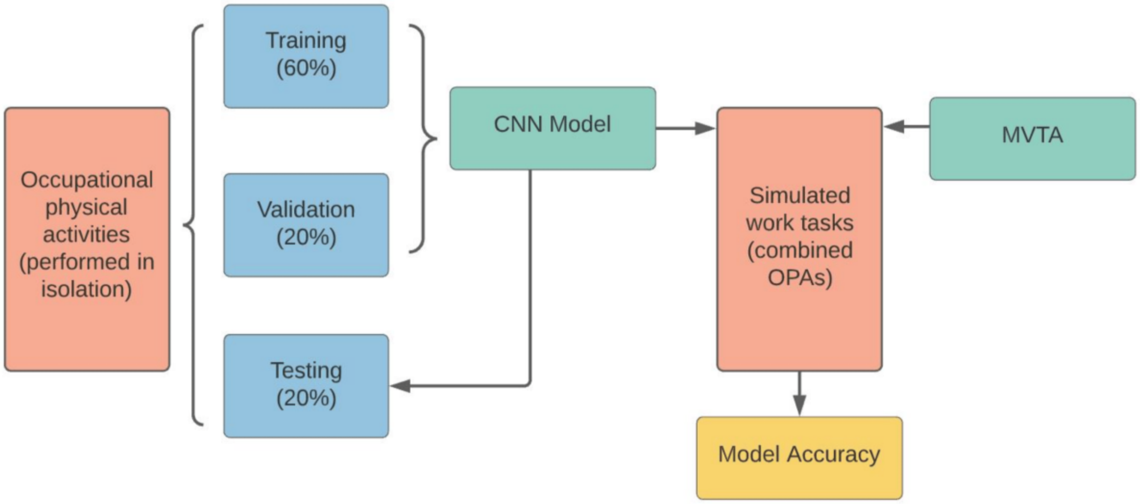

Figure 2-5 This diagram shows the approach for assessing the accuracy of the CNN model. Data collected from the OPAs performed in isolation were divided into 60%, 20%, and 20% for training, validation, and testing, respectively. The trained model was applied to testing data from the OPAs performed in isolations, then the simulated work tasks to predict OPAs. Multimedia video task analysis was performed on the simulated work tasks and compared with model predictions to estimate the accuracy of the predictive model.

2.2.8 Post Hoc Analysis

For the simulated work tasks, the best three CNN OPA predictions each second were compared with the actual OPA identified by MVTA. For the best three CNN predictions of each second, if there was a correct prediction, it was counted. If all three were incorrect, the first OPA prediction was counted as the incorrect prediction.

2.3 Results

A total of 15 healthy participants with an average age of 31 ± 13.6 years (9 males, 6 females, Table 2-3) participated in this study. The average height and weight of individuals were 169.4 ± 14.8 cm and 68.2 ± 15.6 kg, respectively. None of them reported any recent injuries or chronic diseases.

Table 2-3 Demographics and anthropometric data of subjects

Gender	N		Age (yrs)	Height (cm)	Weight (kg)	BMI (kg/m$^{2)}$	Lower leg (cm)	Upper leg (cm)	Lower arm (cm)	Upper arm (cm)
Male	9	Mean	31	177	76.10	24.30	57.44	92.00	37.67	38.89
		SD	15.43	12.13	15.43	4.30	3.68	6.54	2.87	3.26
Female	7	Mean	33	165	61.16	22.45	52.17	85.67	33.33	34.33
		SD	15.79	4.40	7.11	1.75	2.64	2.42	1.97	2.34

The CNN achieved an overall accuracy of 95% in test data but differed by OPA with one handed lifting/lowering having the lowest accuracy (83%) and six OPAs having an accuracy of 100% (Table 2-4).

Table 2-4 CNN model accuracy of different OPA categories (N = number of correct predictions over total samples for each OPA. Accuracy is the percentile of correct predictions divided by total samples)

OPA Category	N of correct samples (windows)	Accuracy
Overhead work	194/194	100%
Sitting	97/97	100%
Crawling	78/79	98%
Standing	103/103	100%
Carrying	271/271	100%
Walking	101/106	95%
Pushing	170/180	94%
Reaching	279/279	100%
Static stooping	84/84	100%
Kneeling	84/85	98%
Crouching	85/96	88%
Lifting/Lowering	1028/1064	96%
One-handed lifting/lowering	273/327	83%
Pulling	80/94	85%
One-handed pulling	194/207	93%
Overall	3121/3266	95%

The data collected from bottle packaging tasks, carpet laying tasks and drilling tasks were combined and processed by the trained CNN model. The top CNN OPA prediction was compared with MVTA results for each frame to calculate the prediction accuracy (Table 2-5). Based on the 1503 frames, the average accuracy was 22% with accuracies varying by OPA. The lowest accuracy was 0% (one-handed lifting) and the highest accuracy was 95% (overhead work).

Table 2-5 Accuracy of the top OPA prediction during simulated work tasks. The confusion matrix shows the CNN model accuracy of OPA predictions in simulated work tasks. OPAs were classified as upper body kinematics or whole-body kinematics. Cells in the left-hand column represent OPA categories in tasks and cells in the second row represents CNN predicted activities. Cells on the main diagonal and off-diagonal indicate the number of correct and incorrect predictions of each activity. Cells marked in darker green represent more predicted numbers. The two right-hand columns represent the total frame and prediction accuracy of each OPAs, respectively. The cell at the bottom-right corner indicates the average prediction accuracy.

	Upper Body Kinematics								Whole Body Kinematics								
OPA Category	Reaching	Carrying	Lifting	Lifting onehanded	Pulling	Pulling onehanded	Pushing	Overhead work	Standing	Walking	Kneeling	Crouching	Crawling	Stooping	Sitting	Total (Frame)	Accuracy
Reaching	**31**	23	47		1	14	1	50		5	7	26	28	1	9	243	13%
Carrying	1	**36**	9			8	11	3		11	1	24	5	5	1	115	31%
Lifting	6	32	**28**			29	16	12		15	8	39	21		3	209	13%
Lifting onehanded		2	5	**0**		7	1	1		3	4	8	3		1	35	0%
Pulling			1		**13**	13	6			2		4				39	33%
Pulling onehanded			1			**0**	1					1				3	0%
Pushing			3		2	29	**23**					2				59	39%
Overhead work			0			0		**40**		1		1				42	95%
Standing	5		21		4	7		1	**17**		4	4	3	1	2	69	25%
Walking	2	8	13		2	14	2			**21**	3	25	4		2	96	22%
Kneeling	1	1	25		2	35	16	1		1	**2**	89	60		4	237	1%
Crouching	7	3	85			1	5			1	7	**24**	13	12	22	180	13%
Crawling			2			2	1					5	**7**			17	41%
Stooping	5	2	33			7	5					9	5	**90**	3	159	57%
Sitting															**0**	0	N/A
Total	58	107	273	0	24	166	88	108	17	60	36	261	149	109	47	1503	22%

The analysis of the three best CNN predictions was higher; the average prediction accuracy was 45% (Table 2-6). Some OPA prediction accuracies were high; accuracy of one-handed pulling and overhead work exceeded 95%, while the accuracy for pushing reached 88%. However, the prediction accuracy of other OPAs was very low. For example, kneeling had an accuracy of 7%, being commonly mistaken for crouching (Figure 2-6). None of the one-handed lifts were correctly predicted. Many frames of stooping were predicted as reaching.

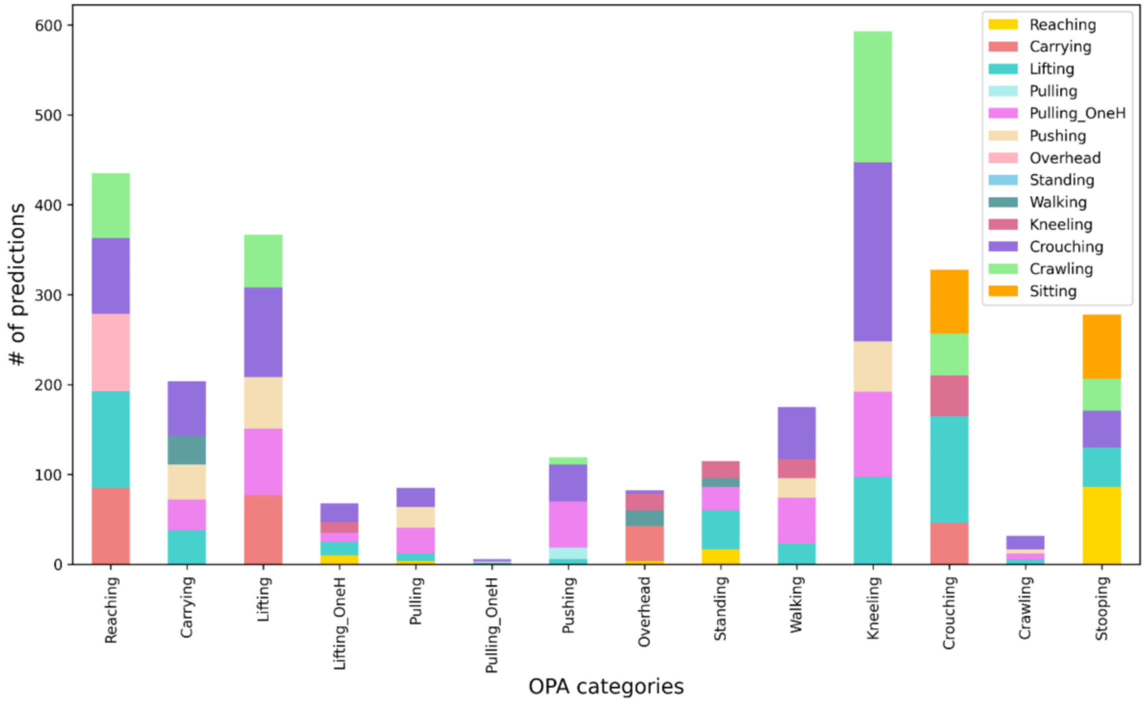

Figure 2-6 This stacked bar chart shows the top 5 other OPAs that each activity was misclassified as. The X-axis represents the OPAs performed during the simulated work tasks and the legend represents OPAs predicted by CNN.

Table 2-6 Accuracy of the top 3 OPA predictions during simulated work tasks. A confusion matrix showing the accuracy of the best three CNN predictions of OPAs in simulated work tasks. If there was a correct prediction in the best three outcomes, the correct one was counted. Otherwise, the first outcome of the best three predictions was counted. Cells in the left-hand column represent OPA categories in tasks and cells in the second row represent the best three predicted activities. The best three CNN predictions of each frame were taken for analysis. Cells on the main diagonal and off-diagonal indicate the number of correct and incorrect prediction of each activity. The two right-hand columns represent the total frame and CNN best three prediction accuracies of each OPA, respectively. The cell at the bottom-right corner indicates the average accuracy of best three CNN predictions.

	Upper Body Kinematics								Whole Body Kinematics								
OPA Category	Reaching	Carrying	Lifting	Lifting onehanded	Pulling	Pulling onehanded	Pushing	Overhead work	Standing	Walking	Kneeling	Crouching	Crawling	Stooping	Sitting	Total (Frames)	Accuracy
Reaching	**103**	20	28		1	14	1	30		4	4	23	9	1	5	243	42%
Carrying	1	**66**	1			6	8			6	1	19	4	2	1	115	57%
Lifting	3	14	**106**			22	11	1		12	4	23	12		1	209	51%
Lifting onehanded		2	5	**0**		7	1	1		3	4	8	3		1	35	0%
Pulling			1		**21**	7	4			2		4				39	54%
Pulling onehanded						**3**										3	100%
Pushing			1			6	**52**									59	88%
Overhead work								**41**		1						42	98%
Standing	1		11		3	5		1	**39**		1	4	3	1		69	57%
Walking	2	4	12		2	6	1			**40**	3	20	4		2	96	42%
Kneeling	1	1	23		2	35	16	1		1	**16**	87	51		3	237	7%
Crouching	7	1	50				4			1	4	**71**	9	12	21	180	39%
Crawling			1				1					3	**12**			17	71%
Stooping		2	33			7	4					9	3	**99**	2	159	62%
Sitting															**0**	0	N/A
Total	118	110	272	0	29	118	103	75	39	70	37	271	110	115	36	1503	45%

2.4 Discussion

The present study used a deep learning method to predict 15 OPA activities common in MMH jobs. A convolution neural network model was applied to data from 8 IMUs to predict which of the 15 OPAs were being performed during each second of analysis. Overall, the model had an average accuracy of 95% when each OPA was performed in isolation. However, model accuracy decreased when applied to simulated work tasks that contained multiple OPAs (e.g., bottle packaging, carpet lying and drilling).

The CNN model was first applied to predict occupational physical activities performed in isolation. The study indicated that the CNN model provided a reliable prediction of OPAs performed in isolation with the highest accuracy of prediction reaching 100%, and the lowest accuracy being 83%. However, even when performed in isolation, some activities had better accuracy than others; overhead work, sitting, standing, carrying, reaching and static stoop had 100% accuracy while one-handed lifting, pulling and crouching were lower (83%, 85% and 88%, respectively). One possible reason for the lower accuracy in one-handed lifting (83%) was the asymmetrical movement that varied with each lift (Figure 2-7a). Pulling and one-handed pulling also had lower prediction accuracy (85% and 93%, respectively) which may have also been due to activity being asymmetrical and varied. The model accuracy for crouching may have been lower (88%) due to the trunk angle being similar to other activities, such as lifting and kneeling. Future studies should include IMU data from the lower legs to evaluate whether additional IMU data improves model prediction for all OPAs by differentiating activities with similar upper body postures (Figure 2-7b).

(a) (b)

Figure 2-7 Activities with similar trunk flexion have low prediction accuracies：(a) one-handed lifting, an asymmetrical activity (83%); (b) crouching (88%).

To test the robustness of the trained CNN model, it was applied to data collected during three MMH tasks. The overall model accuracy fell dramatically to 22%. Each task contained multiple OPAs and the model was unable to differentiate the OPAs with high accuracy when they were performed as part of a simulated task. To understand the inaccurate predictions, a post hoc analysis analyzed the best three CNN predictions for each second of simulated work. The overall accuracy of OPAs increased from 22% to 45%. The results of some activities improved greatly; prediction for lifting and pushing increased from 13% to 51% and 39% to 88%, respectively. This indicates that the model may have had an incorrect best prediction, but the 2nd or 3rd prediction was correct, at least for some OPAs. However, some activities had minimal changes in accuracy. The incorrect predictions for each OPA were graphed to visually depict erroneous predictions for each OPA. This was primarily done to develop improved models for future research, particularly for the OPAs with a low prediction accuracy. Upon further analysis, the erroneous predictions appeared to be primarily due to four circumstances including (1) variation in how the OPA was performed; (2) OPAs being performed concurrently; (3) posture similarities between OPAs; (4) an OPA being embedded in another OPA, thus confusing the model.

The amount of variation in how activities were performed impacted the model prediction accuracy. For example, the CNN model was trained with people lifting using a squat technique, yet during the work simulated tasks, some people used the stoop lift posture which was mistakenly predicted as crouching. Kneeling only had a 7% accuracy despite using the best three predictions. Kneeling can also be performed with much variation; there was kneeling while sitting on the heels, kneeling upright (no hip flexion) and single knee kneeling. Since the model was not trained for these variations in posture, it predicted other similar activities such as crouching or crawling. Future research should include more variations of how each OPA is performed during the training-test dataset before it is applied to simulated work tasks. Fifteen subjects participated in the current study. Including more people in the training-test dataset would also be helpful in capturing variations in how OPAs are performed.

Another reason for poor prediction accuracy was that subjects often performed multiple OPAs at the same moment while performing a task which the single model prediction approach could not resolve. For example, subjects may reach while kneeling, sitting, or standing. Standing was misclassified as lifting since subjects usually lift items when standing. This presented challenges for the CNN model in predicting the predominant activity. Despite the extensive training, evaluation, and discussion about how to classify each frame in MVTA, human judgement was used to identify the predominant activity.

As described above when OPAs were performed in isolation, similar postures across OPAs were a reason for poor accuracy during the MMH tasks, especially since there was no information on loads being handled. Reaching was frequently predicted as lifting, overhead work, and carrying likely because those activities include shoulder flexion with an increased horizontal distance between the body and wrists. Kneeling was commonly misclassified as crawling or crouching, also likely due to the similarities in hip flexion and trunk angles, particularly when kneeling while sitting on one’s heels. Crouching was misclassified as lifting or sitting, again due to similar hip flexion angles. Surprisingly, walking had low prediction accuracies and was most commonly misclassified as one-handed pulling, carrying, or pushing, all of which include walking while handling a load. Having additional information from lower extremity IMUs and/or about loads being handled may improve the OPA classification across these otherwise similar activities that all included some amount of reach.

Another common reason for misclassification was when one OPA was part of or embedded within another OPA. For example, when categorizing OPAs in MVTA, the visual cues made it obvious when someone was reaching forward to lift something. In this case, the lift started at the beginning of the reach to lift an item and ended when the item was brought back to their body. In other words, if someone was reaching forward to lift something, the frames including the reach forward required to make contact with the object, were classified as part of the lift. Despite this consistency in how the models were trained, the CNN model could not differentiate these activities during the simulated activities, based on intent of the movement. This may explain why reaching was incorrectly predicted as a carry and why standing was frequently misclassified as lifting. Thus, a different approach to OPA classification will be needed in the future to help differentiate OPAs. It may be beneficial to start the classification of a lift when the load is actually being lifted versus the moment someone reaches forward to initiate a lift.

To mitigate the misclassification discussed above and improve the prediction accuracy, additional IMUs and/or pressure insoles could be added to the system in future studies. For example, pressure insole information may help differentiate similar activities that primarily differ based on loads being handled such walking versus carrying, pushing or pulling and crouching versus lifting. Information from pressure insoles has been shown to distinguish such activities (Antwi-Afari et al. 2018) and may help distinguish kneeling, crouching, and stooping from lifting. Pressure insole information may also help distinguish crawling from kneeling and crouching since the total force would be significantly lower since the weight is supported through the knees when crawling.

To address concurrent OPAs happening simultaneously, sequential modeling could be used to make multiple predictions. A prior study used sequential artificial neural network models to estimate hand posture before estimating hand exertion force (M. Wang et al. 2020). Perhaps a similar approach that predicts whole body posture before predicting upper extremity movement could be used to improve OPA prediction accuracy.

Continual challenges to estimating prediction accuracies remain because of the transitional time between OPAs when performing simulated work. This can be minimized by training models to make accurate predictions from the beginning of the activity to the very end. For example, lifting would need to be predicted from the first moment there is hip and knee flexion to the moment the person returns to standing. This has obvious challenges for a model that makes a prediction every second and will require proceeding information for accurate classification. Exploring additional types of deep learning models may help to address this issue and improve prediction results. In this study, a recurrent neural network (RNN) model was first applied to predict OPAs when performed in isolation. The prediction result of the RNN model did not meet expectations.

Upon reflection, RNNs are designed to predict an outcome for each timestamp in a time series that was not the best fit for OPA classification. Further, CNN Resnet models have been shown to outperform other deep learning approaches significantly for time series classification (Ismail Fawaz et al. 2019). Thus, the current model chosen for this study was from ImageNet contest winner, Resnet. Its 18-layers implementation is robust to train the model efficiently and retain high accuracy for single OPAs prediction. The window size of the current CNN model was 60 rows of sensor data, roughly corresponding to 1 s of video data which is enough for a single activity to be repetitive and recognizable. However, in MMH tasks, activities change at a very fast pace. Thus, further investigation on window size selection is needed.

2.5 Limitations

Subjects could choose how they performed the simulated work tasks, therefore, some activities such as one-handed pulling and crawling had limited data. For some OPAs like crawling, this may have led to the low accuracy rate, specifically because crawling is similar with other OPAs. Future studies should include more participants and data from a greater number of simulated tasks. Fifteen subjects participated in this pilot study which allowed us to assess the feasibility and accuracy of this approach. In future studies, more subjects will be included to allow more variability when training the model.

2.6 Conclusion

Fifteen occupational physical activities were predicted using a convolutional neural network model and inertial measurement units with an overall accuracy of 95% when performed in isolation, however, the prediction accuracy was low and varied widely when applied to simulated work tasks that included multiple OPAs. Reasons for the reduced accuracy may be addressed in future studies by exploring sequential modeling approaches, model selection, and the addition of lower extremity IMUs and/or pressure insole sensors. Predicting OPAs using wearable devices and deep learning models is an important step in quantifying physical job demands with more accuracy than current methods.

3 Phase II: Comprehensive Recognition of OPAs

3.1 Introduction

As discussed in Chapter 1 and 2, physical demand analysis is a critical component of recruitment, placement, and return-to-work programs. A key aspect of PDA involves identifying occupational physical activities, especially high-risk tasks, helping employers prioritize targeted interventions, optimize workflows, and implement effective ergonomic solutions that enhance workplace safety and reduce injury risks.

Accurate quantification of OPAs, as highlighted in Chapter 2, is essential for determining whether job demands are within safe limits for workers. This data helps design safer jobs, reducing the risk of WMSDs and promoting a healthier work environment. Historically, self-reports, observational techniques, and direct measurements have been used to quantify OPAs. Self-reports, such as questionnaires, are common in large field studies due to their simplicity and cost-effectiveness but are prone to imprecise and unreliable results stemming from random errors and reporting biases (Olds et al. 2019; Ainsworth et al. 2012). While convenient and inexpensive, observational techniques may be resource-intensive and require trained personnel to ensure accuracy (Takala et al. 2010). Direct measurement methods, though more reliable, can disrupt work activities and be impractical for certain tasks.

Advanced technologies have been employed as effective methods to achieve more precise and reliable quantification of OPAs. Several studies have used video-based techniques to identify occupational postures (>80%) accurately (Zhang, Yan, and Li 2018; X. Yan et al. 2017; Escorcia et al. 2012). However, video-based methods face limitations in natural work environments, as their performance can be affected by lighting, self-occlusion, and occlusion from the work environment (Lin et al. 2022; Rodrigues et al. 2022). Wearable devices, particularly inertial measurement units (IMUs), are increasingly utilized to measure kinematic data, including position, velocity, and acceleration of body segments. IMUs have been applied to quantify physical activities in daily living and, more recently, to OPAs in workplace settings (Mäkela et al. 2022; J. Chen, Qiu, and Ahn 2017; Humadi et al. 2021b; Villalobos and Mac Cawley 2022).

Despite these advancements, applying these methods to recognize OPAs in real-world settings while multiple activities are involved remains challenging. The complexity arises due to the simultaneous performance of multiple activities, intraclass variability, interclass similarity, and the overall diversity of work tasks (K. Chen et al. 2020; Nematallah and Rajan 2024). In Phase I (Chapter 2), we utilized eight IMUs and a CNN model to recognize 15 OPAs when activities were performed in isolation and as sub-activities within simulated work tasks. The study achieved 95% accuracy when OPAs were conducted in isolation. However, the accuracy dropped to 22% when activities were performed concurrently as sub-activities in the simulated work tasks (Y. Yan et al. 2021). Specifically, users often engage in several concurrent and interleaving activities (Okita and Inoue 2017; Hao Hu et al. 2008). However, most current studies, as highlighted in prior research, are designed to label only a single activity for each time point. For example, a participant lifting an item from the ground will have a lifting posture in their upper body. In contrast, their whole-body posture could be categorized as crouching or stooping, causing this movement to belong to two activity categories.

To address the challenges of classifying simultaneous activities, Bonde et al. used geophone sensors to classify activities into two categories based on their potential to overlap. By applying multi-stage supervised learning, their system achieved up to 97% accuracy for the first category and up to 90% for the second category and overlapping activity combinations (Bonde et al. 2020). Okita et al. developed a compositional CNN-LSTM (Convolutional Neural Network, Long Short-Term Memory) model capable of recognizing up to three overlapping activities, addressing the limitation of traditional models that detect only one activity at a time. This approach improved recognition accuracy from 27% to 43% (Okita and Inoue 2017). However, these studies primarily focus on office or daily human activities with a limited set of categories, which may not fully capture the complexity and diversity of OPAs. In Phase II, we aim to enhance the accuracy and reliability of recognizing simultaneous OPAs in real-world tasks.

Therefore, the objective of this study was to use wearable technology, specifically IMUs, to provide a more reliable and valid approach for recognizing occupational physical activities related to MMH tasks. Seventeen IMUs were used to measure kinematic data, while deep learning models were employed to recognize whole-body and upper-body activities separately. By accurately identifying these activities, we can enable comprehensive and scalable risk assessments, facilitating a whole-job analysis rather than focusing solely on individual movements. This broader approach is essential for developing effective interventions and improving workplace safety and health.

3.2 Methods

3.2.1 Participants and Devices

This was a laboratory-based study that included thirty participants who were recruited via email, campus announcements, and personal networks. Inclusion criteria required participants to be between the ages of 18 and 65, and physically capable of performing moderate physical tasks. People with neck, back, arm, or shoulder injuries were excluded from the study. Eligible participants were provided with an overview of the study and written informed consent was obtained. This study was reviewed and approved by the University of California.

Seventeen wireless lightweight (16g) and compact (47 mm × 30 mm × 13 mm) IMUs (MVN Awinda and MVN Analyze, Xsens, Netherlands) were attached to participants' feet, lower legs (tibia close to the knee), upper legs (middle of the lateral thigh), pelvis, shoulders, sternum, head, upper arms (between the biceps and the triceps), forearms (closer to the wrist), and hands to capture body kinematics during various activities (60 Hz sampling rate). Two cameras were placed perpendicular to the participants from the right and left sides to ensure clear visibility of key body segments during lifting activities in front of a shelf (Figure 3-2). Additionally, when participants performed all other OPAs, the researcher used a handheld GoPro camera for video recording. The videos were synchronized with the collected IMU data by identifying designed movement patterns at the beginning of each recording.

3.2.2 Study Procedure

By referencing the physical demands outlined by the U.S. Bureau of Labor Statistics ("Visual Overview for Physical Demands"), thirteen OPAs commonly associated with MMH jobs were selected for our study. The 13 OPAs (Table 3-1, Table 3-2) were performed in isolation by each participant while wearing all 17 IMUs. The kinematic data were used to train a deep-learning model to recognize whole-body and upper-body activities separately. The trained model was tested to recognize activities when performed as sub-activities in simulated work tasks that mimicked real-world tasks. Multimedia video task analysis (MVTA) was used to analyze videos of simulated tasks frame by frame and compare them with results from the deep learning model to calculate the percentage of correctly predicted activity periods (Figure 3-1). Leave-group-out cross-validation (CV) was conducted to assess whether the model could maintain similar performance both with participants previously included in the model and with new, unseen participants on recognizing their OPAs (dashed line in Figure 3-1).

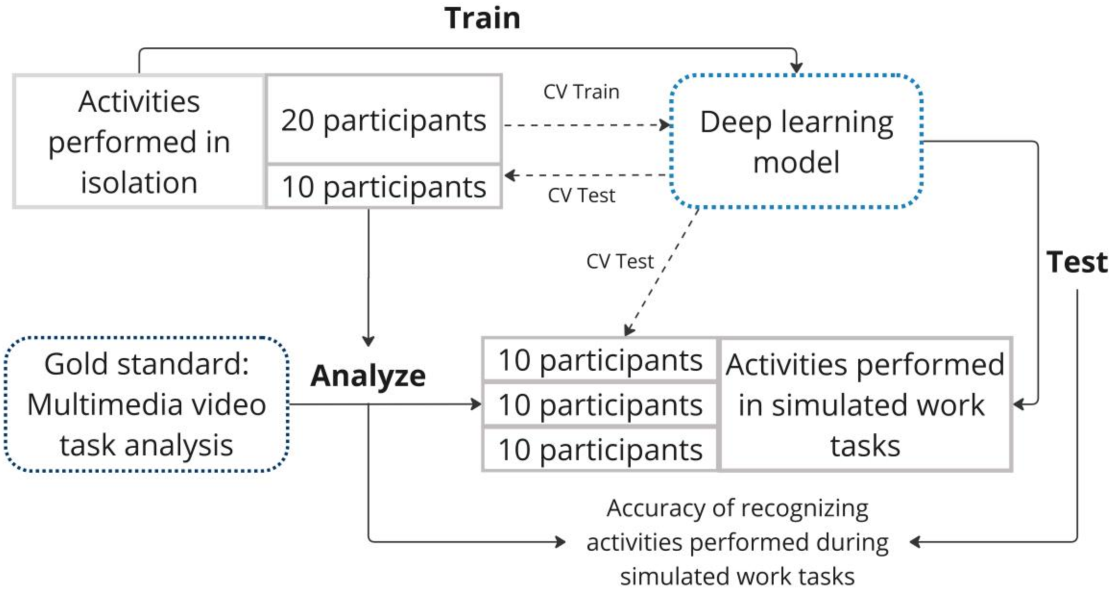

Figure 3-1 The study procedure for occupational physical activity recognition uses inertial measuring units and a deep learning model.

3.2.3 Occupational Physical Activities

The 13 OPAs included seven whole body activities (sitting, standing, walking, symmetrical kneeling, asymmetrical kneeling, crouching, and stooping) and six upper body activities (reach high, carrying, pushing, pulling, lifting, below shoulder non-MMH movement). Each participant performed most whole body activities for at least one minute (once) without additional weight. Asymmetrical kneeling was performed on each knee for 30 seconds. Participants were encouraged to adjust their posture, even while performing a specific whole body activity. For example, during sitting, participants could lean forward, lean back in the chair, cross their legs, etc. Additionally, participants performed crouching with three different postures: deep squat, mid squat, and high squat, which was characterized by knee and trunk flexion angles. Participants adjusted trunk flexion angle for stooping while keeping their knees close to a neutral position.

Table 3-1 Whole body occupational physical activity categories, including the number of repetitions, and the duration of each repetition for each activity.

OPA Category		Repetition Duration	Repetition
1	Sitting	1 min	1
2	Standing	1 min	1
3	Walking	1 min	1
4	Kneeling	1 min	1
5	Asymmetrical Kneeling	30s	2
6	Crouching	1 min	1
7	Stooping	1 min	1

Table 3-2 Upper body occupational physical activity categories, including the load handled, the number of repetitions, and the duration of each repetition for each activity.

OPA Category	Load	Repetition Duration	Repetition
Reach High	Driller	1 min	1
Carrying	5 kg, 7kg, 10 kg (box)	1 min	3
Pushing	Initial force: 4.5 kg; Sustained force: 2.7 kg Initial force: 5.4 kg; Sustained force: 3.6 kg (cart)	NA	12
Pulling	Initial force: 4.5 kg; Sustained force: 3.2 kg Initial force: 5.4 kg; Sustained force: 4.5 kg (cart)	NA	12
Lifting	2 kg, 5 kg, 7 kg (box)	NA	115
Below Shoulder Non-MMH Movement	NA	1min (below shoulder reach) NA	NA

A drill was used during the "Reach high" activity for upper body activities to simulate overhead drilling. Participants carried three boxes with handles (5kg, 7kg, and 10kg) for 1 minute each. Two weights were placed on a cart during pushing and pulling tasks, and the initial and sustained forces were measured (Table 1). Participants pushed and pulled the cart across the room without a time limit. Each activity was repeated 12 times (6 times per weight). Participants also performed a series of lifts (up to 115 per participant) using three loads (2kg, 5kg, and 7kg). The boxes, marked with different colors to indicate their weights, were lifted to and from shelves with various heights (floor, 76.2cm, and

152.4cm) and locations (left and right), resulting in 6 distinct locations (Figure 3-2). Floor markings indicated where participants should stand to start each lift, varying the horizontal hand location. During the lifting activity, participants were instructed to move boxes between specified locations sequentially. Lifting parameters were determined based on the revised NIOSH equation to accommodate standard lifts in manual material handling and prevent participant injuries.

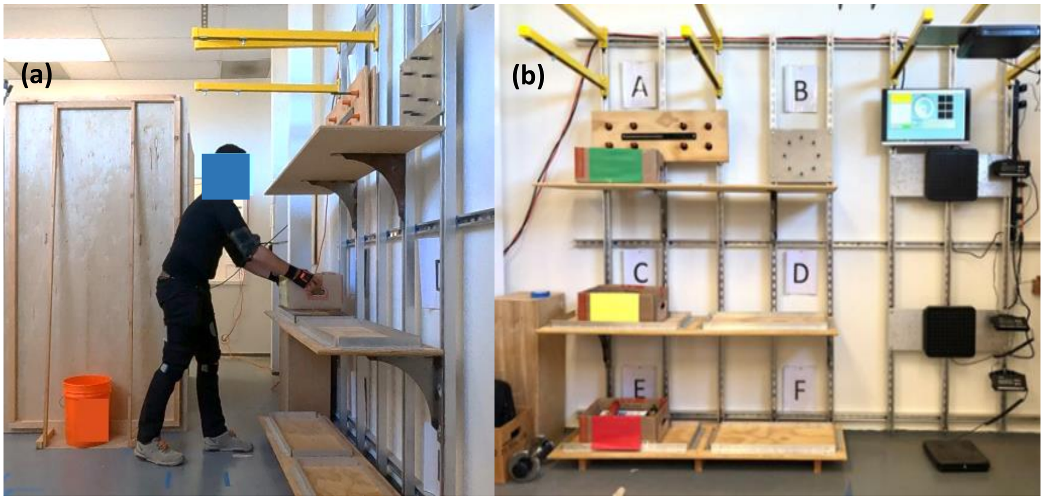

Figure 3-2 Lifting activities are performed in front of a shelf. (a) A participant lifts a box from the shelf while wearing sensors recorded by a GoPro camera. (b) The shelf has six locations (left/right × 3 vertical shelf heights).

3.2.4 MMH Tasks

Three simulated work tasks were designed to encompass all thirteen occupational physical activities (Figure 3-3). Participants received verbal instructions before starting the tasks and reminders during the functions. Physical demonstrations were provided only upon the participant's request.

Object sorting: Each participant sorted penny rolls and weights into two separate baskets. The participant lifted and carried the first basket (2kg), placing it on one of the three shelves. Then, the participant walked back, lifted and carried the second basket (5kg), and placed it on another shelf. Finally, the participant returned, lifted, and carried a box with weights (7kg) and placed it on the remaining shelf height.

Carpet laying: Each participant lifted 12 carpets (4 times in total: 4, 4, 2, 2) onto a cart. The participant then pushed and pulled the cart to the designated location, lowered the carpets to the ground, and knelt to lay the 12 carpets in the specified area. Then, the participant pushed and pulled the cart back to its original location.

Drilling: Each participant performed drilling tasks in multiple positions, including drilling overhead while standing, drilling in front of the body while stooping or in a deep crouch position, and drilling on the ground while kneeling on one knee.

Participants completed the object sorting and carpet laying tasks at their own pace without any time constraints. Each movement was performed for a minimum of 40 seconds for the drilling task. For each frame, every movement performed during the three tasks could be classified into one whole-body and one upper-body activity by MVTA.

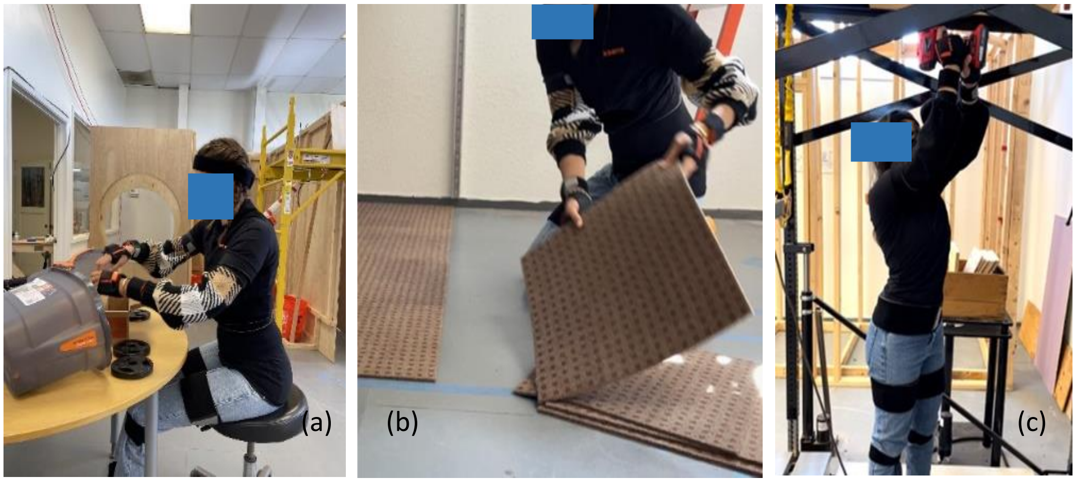

Figure 3-3 Participants performing MMH task (a) Participant sorting penny rolls into baskets with a whole body activity of sitting and an upper body activity of below-shoulder non-MMH movement; (b) Participant laying carpet on the ground with a whole-body activity of kneeling and an upper-body activity of below-shoulder non-MMH movement; (c) Participants drilled above with a whole-body activity of standing and an upper-body activity of reaching high

3.2.5 Model Training and Testing

3.2.5.1 Activity Recognition in Isolation

A 2D Convolutional Neural Network (CNN) ResNet-18 architecture was used to train two models: one to recognize whole-body activity and a second for upper-body activity recognition.

Data preparation:

Kinematic data, including triaxial position, velocity, acceleration of various body segments, and joint angles (e.g., abduction/adduction, flexion/extension), were collected using seventeen IMU sensors and processed with Xsens MVN Analyze (sampling rate = 60Hz). All velocity features were converted into the xy plane and used as model inputs.

Given that individuals can assume various upper-body postures while performing a single whole-body activity (e.g., standing while lifting or performing below-shoulder non-MMH movements), it was crucial to minimize the influence of movement from the upper extremity on whole-body activity recognition and vice versa. Additionally, extracting appropriate features depended on the application domain, making it essential to retain relevant information (Mo et al. 2016). Therefore, feature selection was further refined based on kinematics and researchers' validation:

- Whole Body Recognition Model: Features from the lower extremity and pelvis were used as model inputs, totaling 32 input features.
- Upper Body Recognition Model: Features from the upper extremity were used as model inputs, totaling 46 input features.

The selected features were transformed into fixed-length, non-overlapping, image-like windows, with each row representing a different feature and each column representing a frame in the time series. Each window contained 60 columns, representing 1 second of collected data. The OPA categories were added to the selected data for seven whole body and six upper body activities as the activity’s label. For model training, only windows with a single activity were included. Thus, each row contained 1 column for the timestamp and 1 column for the activity label in addition to the input features.

Model Training:

Processed data was divided into 60% for training, 20% for validation, and 20% for testing. The models were trained using the Adam optimizer with a learning rate of 0.001 and a batch size of 32. To determine convergence, training ended when there was no improvement in the validation set within five consecutive epochs. Regularization techniques, including a dropout layer with a probability of 0.5, were applied to prevent overfitting. Cross-entropy loss was used as the loss function, with error defined as the average cross-entropy loss over all samples in a batch. Upon completion of training, the best model was selected based on its performance with the validation data.

3.2.5.2 Activity Recognition in Simulated Work Tasks

Kinematic data were collected from simulated work tasks and processed into image-like windows representing 1 second of data, similar to the isolated activities. The models trained on isolated activities were then employed to separately recognize whole- and upper-body activities performed during each second of the simulated work tasks.

Multimedia video task analysis (MVTA) was used as the gold standard to accurately identify performed activities during the tasks. This method allows for the interactive identification of events using breakpoints in videos. Trained researchers used MVTA to analyze videos of work tasks. Videos were analyzed twice, the first to identify whole-body activities and the second time to identify upper-body activities. Researchers inserted breakpoints whenever a change in activity was observed. If a window contained multiple activities (e.g., the participant changed from standing to walking within one second), the window was relabeled with the activity that occupied a larger percentage of the second. Consequently, each second of the entire task was labeled for both whole- and upper-body activities. The model recognition results (predicted class) were then compared with MVTA results (true class) to evaluate model precision based on the exactness of the classifier and recall or sensitivity, which represents the model's ability to identify instances of each activity correctly:

$$Precision = \; TP/(TP + FP) \tag{3-1}$$

$$Recall = TP/(TP + FN) \tag{3-2}$$

Where TP: True positive; FP: False positive; FN: False negative.

3.2.5.3 Leave-group-Out Cross-Validation

In Human Activity Recognition datasets, samples from the same subject are likely related due to underlying environmental, biological, and demographic factors. Therefore, we employed leave-group-out cross-validation, which splits the training and testing sets by subjects (Figure 3-4).

Leave-group-out cross-validation ensures that data from the same subject does not appear in the training and testing sets, thereby providing a more realistic assessment of the model's performance on unseen subjects. Thirty subjects were randomly divided into three groups. For each iteration of the cross-validation process, the whole-body and the upper-body activity recognition models were trained on data collected from isolated activities performed by two of the three groups. Then, the model was initially tested on isolated activities from the third, unseen group. Subsequently, the same trained model was evaluated using the simulated work tasks performed by the third group, ensuring that all subjects' data were used once for testing. This two-step testing process—first on isolated activities and then on simulated work tasks—provided a robust assessment of the model's generalizability and performance.

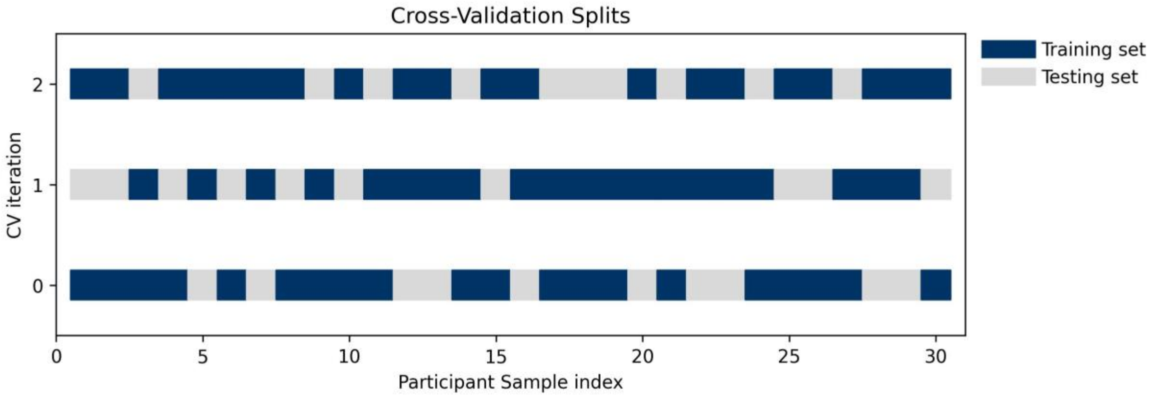

Figure 3-4 Leave-group-out cross-validation with three groups, each consisting of 10 subjects

3.3 Results

Thirty participants (18 females and 12 males) with an average age of 28.3 years (SD = 8.2) participated in this laboratory study. None of the participants reported any recent injuries or chronic diseases.

3.3.1 Whole body activity recognition

Isolated Activities:

Participants (n = 30) performed whole body activities in isolation, with data collected over 3 hours and 57 minutes. Data segments where multiple activities occurred within the same second were excluded (1.41%), leaving 3 hours and 54 minutes of usable data for training, validating, and testing the whole-body activity recognition model. The model achieved an overall accuracy of 99.1% for activities in test data when performed in isolation, with stooping having the lowest recall at 97.9% (Table 3). All windows of (symmetrical) kneeling were correctly recognized.

Simulated Tasks:

Participants performed three simulated tasks, resulting in approximately 3 hours and 41 minutes of collected task data. None of the data windows were dropped, and the trained whole-body activity recognition model achieved an overall accuracy of 89.0% (Table 4). Walking achieved the highest recall at 96.0%, with a few misclassifications into standing, crouching, and stooping. Standing had the lowest recall at 78.2%, with several instances misclassified as walking and crouching. The model demonstrated high effectiveness for kneeling and sitting, with precision values of 97.8% and 94.0%, respectively, indicating a high rate of correct predictions when these activities were identified

Table 3-3 Whole body activity recognition results for isolated activities

Whole-body Activities	N of correct windows	Recall
Sitting	377/378	99.7%
Standing	378/382	99.0%
Walking	414/420	98.6%
Kneeling	423/423	100.0%
Asymmetrical kneeling	418/419	99.8%
Crouching	404/408	99.0%
Stooping	371/379	97.9%
Total	2785/2809	99.1%

Table 3-4 Confusion matrix of whole body activity recognition during simulated work tasks

		Predicted Class							
	OPA category	Sitting	Standing	Walking	Kneeling	Asymmetrical Kneeling	Crouching	Stooping	Recall
True Class	Sitting	**1260**	87	3	10	9	71	0	87.5%
	Standing	2	**1916**	330	0	2	118	82	78.2%
	Walking	0	79	**3378**	0	0	42	20	96.0%
	Kneeling	6	3	12	**1466**	60	18	0	93.7%
	Asymmetrical Kneeling	0	0	2	16	**1122**	82	0	91.8%
	Crouching	72	11	91	7	97	**1571**	50	82.7%
	Stooping	0	19	12	0	0	29	**1142**	95.0%
	Precision	94.0%	90.6%	88.2%	97.8%	87.0%	81.4%	88.3%	Overall Accuracy: 89.0%

3.3.2 Upper body activity recognition

Isolated Activities:

Participants performed upper body activities in isolation, with data collected over 9 hours and 18 minutes. Windows containing multiple activities were dropped (1.7 %), leaving 9 hours and 9 minutes of data for the upper body recognition model. The model achieved an overall accuracy of 98.2% in recognizing the six categories of upper body activities when performed in isolation. All windows of reach high were identified accurately, although pushing had the lowest recall at 94.6%.

Table 3-5 Upper body activity recognition results for isolated activities

Upper-body Activities	N of correct windows	Recall
Reach High	361/362	99.7%
Carrying	1224/1236	99.0%
Pushing	617/651	94.6%
Pulling	614/622	98.7%
Lifting	2389/2411	99.1%
Below Shoulder Non-MMH Movement	1263/1298	97.3%
Total	6438/6556	98.2%

Simulated Tasks:

The data collected from the simulated work tasks were also labeled with upper body activities using MVTA and compared with the trained model for recognizing these activities. Among the three simulated work tasks, the trained model achieved an overall accuracy of 84.8% in recognizing upper body activities. Both pushing and pulling received a recall of over 95.0%, though some were occasionally misrecognized as each other. However, lifting and below-shoulder non-MMH movement had relatively low recall during simulated tasks, with 9.7% of lifting incorrectly predicted as below-shoulder non-MMH movement and 12.8% of below-shoulder non-MMH movement misidentified as lifting.

Table 3-6 Confusion matrix of upper body activity recognition during simulated work tasks

Predicted Class

True Class

OPA category	Reach High	Carrying	Pushing	Pulling	Lifting	Below Shoulder Non-MMH Movement	Recall
Reach High	**1196**	0	1	0	45	29	94.1%
Carrying	0	**464**	15	0	53	4	86.6%
Pushing	0	1	**755**	28	3	3	95.6%
Pulling	0	0	24	**828**	7	9	95.4%
Lifting	2	60	47	2	**1037**	123	81.6%
Below Shoulder Non-MMH Movement	24	103	291	51	1092	**6935**	81.6%
Precision	97.9%	73.9%	66.6%	91.1%	46.4%	97.6%	Overall Accuracy: 84.8%

3.3.3 Leave-group-out Cross-Validation

Each model was trained using data from 20 participants performing isolated activities for both whole-body and upper-body activity recognition approaches with validation testing conducted on the remaining 10 participant. This procedure was repeated three times, and the results were aggregated to calculate the number of correct windows and recall for each activity (Table 3-7, Table 3-8).

For whole body activity recognition (Table 3-7), this approach achieved an overall accuracy of 97.0% during isolated activities and 89.8% during simulated work tasks with new (unseen) users. Although the recall for most whole-body activities was above 90% during isolated activities, sitting, crouching, and standing exhibited relatively lower recall, with standing having the lowest recall of 78.7%.

When recognizing upper body activities (Table 3-8), this approach reached an overall accuracy of 94.8% when activities were performed in isolation and 80.5% accuracy when activities were conducted in simulated work tasks, when tested on unseen users, with below shoulder non-MMH movements having the lowest recall of 75.5%.

Table 3-7 Aggregate results of whole body activity recognition using leave-group-out cross-validation across three runs

Whole body activities	In Isolation		Simulated Work Tasks	
	N of correct windows/Total	Recall	N of correct windows/Total	Recall
Sitting	2035/2134	95.4%	1276/1447	88.2%
Standing	1929/1961	98.4%	1928/2449	78.7%
Walking	2195/2211	99.3%	3401/3511	96.9%
Kneeling	1919/1969	97.5%	1482/1566	94.6%
Asymmetrical kneeling	2106/2123	99.2%	1116/1209	92.3%
Crouching	1836/1933	95.0%	1576/1910	82.5%
Stooping	1793/1914	93.7%	1159/1204	96.3%
Overall Accuracy	13813/14245	97.0%	11938/13296	89.8%

Table 3-8 Aggregate results of upper body activity recognition using leave-group-out cross-validation across three runs

Upper body activities	In Isolation		Simulated Work Tasks	
	N of correct windows/Total	Recall	N of correct windows/Total	Recall
Reach High	1711/1733	98.7%	1197/1269	94.3%
Carrying	6026/6324	95.3%	460/537	85.7%
Pushing	2658/3301	80.5%	699/792	88.3%
Pulling	3002/3160	95.0%	804/880	91.4%
Lifting	11841/12066	98.1%	1082/1274	84.9%
Below Shoulder Non-MMH Movement	6461/6871	94.0%	6403/8479	75.5%
Overall Accuracy	31699/33455	94.8%	10645/13231	80.5%

3.4 Discussions

In this laboratory study, 30 subjects performed 13 OPAs (7 whole body and 6 upper body activities) in isolation and three simulated work tasks. CNNs were employed to recognize whole body activities and upper body activities separately. Overall, the whole body activity model achieved an accuracy of 99.1% in isolation and 89.0% in simulated work tasks. The upper body activity model achieved an accuracy of 98.2% in isolation and 84.8% in simulated work tasks. These accuracies indicate that this approach could reflect the percent time spent in each OPA, as required in a physical demand analysis. Current methodologies estimate the time allocation for an OPA using broad categories—never, occasional (0-33%), frequent (33-67%), and constant (≥67%)—and rely on less precise methods for determining OPA frequency. In this study, all activities, except standing (which had a recall rate of 78.2%), were accurately recognized in over 80% of the time windows (seconds) in simulated work tasks. Overall, this approach would improve the accuracy of OPA allocation.

Although the overall accuracy for recognizing whole-body activities decreased to 89.0% in simulated work tasks, over 90% of walking, kneeling, asymmetrical kneeling, and stooping activities were correctly identified. However, 13.5% of standing instances were misclassified as walking, likely due to participants' tendency to shift their stance by stepping sideways, forward, or backward, which may have been inadequately captured during MVTA and led to challenges in model recognition. Additionally, 4.8% of standing instances were misclassified as crouching, often resulting from transitional movements, such as bending over to lift an item from a lower position.

The recognition of upper body activities had lower accuracy (84.8%) in simulated work tasks than in whole body activities. This reduced accuracy can be attributed to the greater degrees of freedom in upper body joint angles, resulting in a broader range of motion and increased variability in movement patterns. Consequently, significant activity variability and considerable overlap between activities exist. Additionally, the frequent transitions between different upper-body movements required to complete tasks (e.g., sorting items, laying carpets) contribute to extended transition periods between OPAs, further complicating accurate recognition. For instance, carrying activities had a recall rate of 86.6%, with 9.9% of carrying instances misclassified as lifting. The similarity in movement patterns can partially explain this misclassification; when participants were carrying an item, the forward-reaching movement of their arms often resembled a portion of lifting activities, particularly when the start and end locations of the lift were close to the trunk. For example, in the carpet-laying task, participants sometimes lifted the carpet from a cart, took one or two steps toward the designated area, and then dropped the rug onto the ground. These movements share similarities with both lifting and carrying, making it difficult for MVTA to accurately label the movements and challenging for the model to recognize. Additionally, lifting an object from one location, carrying it, and then lifting/lowering it to another is standard. Still, the transition periods between these actions are difficult to categorize accurately.

Both lifting and below-shoulder non-MMH movements had a lower recall rate, approximately 81.6%. Specifically, 9.6% of lifting activities were misclassified as below-shoulder non-MMH movements, while 12.9% were misclassified as lifting. These two categories exhibit high variability. Lifting involves a wide range of hand positions, trunk rotations, and items lifted. This study's simulated work tasks included lifting from the ground a shelf at three different heights, a table, and a cart, with hand posture varying based on whether participants lifted boxes or carpets. However, only boxes lifting from the shelf at different heights were included in isolated activities. Due to the variability in lifting conditions, covering all possible scenarios in the model's training set is impractical. Below-shoulder non-MMH movements encompass a range of actions, including moments when participants were not engaged in arm movement (e.g., standing or sitting with arms in a neutral position) and when they were reaching below shoulder height (e.g., sorting items on a table or laying carpets on the ground), involving a broad spectrum of arm movements. These movements accounted for significant time across the three simulated tasks and were frequently misclassified with lifting.

There were some limitations in the model presented in this study. Notably, the model's precision for lifting and below-shoulder non-MMH movements was less than 50%, which is still much better than random chance, which would be 16.7%. This misclassification primarily occurred during the carpet-laying task, where participants usually dragged or moved carpets close to the ground but sometimes lifted them slightly higher. However, these actions were labeled as below-shoulder non-MMH movements in MVTA due to the subject's whole body posture (kneeling), which is not included in the Revised NIOSH Lifting Equation for ergonomic risk analysis. To address this issue, future work could incorporate whole-body posture recognition as an additional feature to refine the classification. By filtering out mislabeled lifting movements based on whole body postures, we can prevent them from influencing subsequent analyses of true lifting activities and improve overall model accuracy. Another limitation of this study is that the data were collected in a controlled laboratory setting, which may limit the generalizability of the findings. Although the three work tasks we designed were intended to simulate complex real-world tasks, there remains a gap between laboratory conditions and actual workplace environments. Testing this approach with field data from workers in diverse industries would provide a more comprehensive assessment of its applicability.

Leave-group-out cross-validation results revealed a modest decrease in accuracy for recognizing whole body and upper body activities performed in isolation, with recognition accuracy declining from 99.2% to 97.0% for whole body activities and from 98.2% to 94.8% for upper-body activities. However, the effect on whole body activity recognition performance during the three simulated work tasks was minimal. Notably, the accuracy slightly improved from 89.0% to 89.8%, which can be attributed to an increase in recall for the walking activity. In contrast, the upper body activity recognition model showed a slight performance decrease in the simulated work tasks, with accuracy declining from 84.8% to 80.5%. Overall, while applying these models to recognize activities of unseen subjects led to minor reductions in accuracy, the performance remains promising, demonstrating the models' potential for future applications.

In Phase I, a Resnet-18 model was used to recognize 15 occupational physical activities (OPAs) with wearable data collected using 8 IMUs, without separating whole-body activities and upper-body activities. The model achieved a high recognition performance of 95% overall accuracy when each OPA was performed in isolation. However, the model's accuracy decreased to only 22% when applied to simulated work tasks. The significant drop in performance highlighted the approach's limitations in handling concurrent activities, where multiple OPAs are performed simultaneously. In the current study, by employing more IMUs and, more importantly, separating whole body activities from upper body activities, the current method was able to recognize OPAs even more effectively in complicated simulated work tasks. The separation allowed the model to account for the different movement patterns involved in complex tasks.

This study aims to recognize OPAs within more complex simulated work tasks, rather than only in isolation, to enhance its applicability for real-world scenarios. In a study focused on recognizing daily routines rather than simple activities, Huỳnh et al. introduced an approach using topic models to identify complex daily routines as probabilistic combinations of activity patterns (Huynh, Fritz, and Schiele 2008). Hu et al. emphasized the importance of recognizing multiple concurrent and interleaving activities, arguing that real-world behavior often involves overlapping tasks. Their approach employed a Skip-Chain Conditional Random Field (SCCRF) model, which allowed for accurate detection of concurrent actions and recognition of long-distance dependencies within action sequences (Hao Hu et al. 2008). Instead of using probabilistic or skip-chain models, this study focuses on distinguishing between whole body and upper body activities to better address the specific challenges of concurrent actions in occupational settings. This separation is vital for ergonomic assessments, as it allows for more precise recognition of complex task combinations, such as lifting while crouching—a posture that is ergonomically preferable to stooping during low lifts.

In addition to wearable sensor-based methods such as IMUs employed in this study, computer vision-based techniques have also shown advancements in activity recognition. These methods leverage visual data captured by cameras and have demonstrated strong performance in recognizing a variety of human activities. For instance, Khosrowpour et al. demonstrated the use of RGB-D cameras to assess worker activities in construction settings and achieved an average accuracy of 76% in recognizing various construction activities (Khosrowpour, Niebles, and Golparvar-Fard 2014). They noted that camera placement had to be strategically adjusted to capture optimal angles, which introduced additional variability in body posture recognition. Despite their potential, video-based techniques face limitations, including sensitivity to occlusions, variability in lighting conditions, and restricted camera placement, which can impact data quality. In construction environments, workers often interact with materials or are partially blocked by tools and structures, posing challenges for vision-based systems to achieve consistent accuracy. Mo et al. addressed some of these issues by leveraging skeleton data extracted from video sources to minimize the impact of view variance and background complexity (Mo et al. 2016). Nevertheless, challenges such as occlusion, complex interactions, and view dependence continue to affect OPA recognition with video-based techniques in real-world settings.

Wearable sensor-based methods, such as the use of IMUs, offer several benefits for recognizing occupational physical activities. One significant advantage is the ability to provide continuous, location-independent monitoring of body movements. Unlike camera-based systems, which are sensitive to issues such as occlusions, lighting conditions, and the need for strategic placement to avoid blocked views, wearables ensure consistent data collection regardless of environmental conditions or the user’s position.

Besides, wearable devices can also capture detailed data on specific body parts, including joint angles, hand locations and orientations, which are particularly valuable for comprehensive ergonomic risk assessments (Humadi et al. 2021b; Baklouti et al. 2024; Humadi et al. 2021a). For example, precise hand-tracking enables researchers to identify high-risk hand positions and repetitive movements that contribute to musculoskeletal disorders. This functionality extends the role of IMUs beyond activity classification to providing actionable insights that can guide ergonomic improvements in workplace design and task execution.

In the next Chapter (Chapter 4) of the thesis, data segments where workers performed manual lifting were further analyzed. These segments provided critical exposure metrics, such as hand locations and repetition counts, which were used for ergonomic risk assessment using tools like the Revised NIOSH Lifting Equation. Moving forward, exposure metrics for other manual material handling activities, such as carrying, pushing, and pulling, could also be explored for further ergonomic risk assessment. Additionally, future research could investigate methods to minimize the number of IMUs required. Subsequently, exploring the integration of camera data may reveal whether it is possible to further reduce the number of IMUs while enhancing system performance. This approach could involve using a single camera in conjunction with a few strategically placed IMUs, potentially improving data quality while simplifying the wearable system.

Overall, by separating whole body and upper body activities, the model not only improved overall recognition accuracy (around 85% in simulated tasks) but also facilitated more accurate ergonomic risk assessments. This approach provides a more reliable and detailed quantification of OPAs, which is crucial for PDA. By refining the evaluation of activities, the model can significantly contribute to optimizing PDA across various industries, ultimately promoting safer job performance and supporting more informed decision-making in workforce management.

3.5 Conclusions

This study demonstrates the effectiveness of using wearable technologies and deep learning models to recognize and quantify OPAs with high accuracy. The proposed model achieved high accuracy in recognizing OPAs both in isolation (>98% for both whole body and upper body activities) and in complex simulated work tasks (89.0% for whole body activities and 84.8% for upper body activities), highlighting its potential for real-world ergonomic risk assessment. By refining the recognition of manual handling activities such as lifting, carrying, and pushing, the approach provides more precise insights for PDA, which is essential for enhancing workplace safety. Despite challenges such as occasional misclassifications and the constraints of laboratory-based simulations, this study lays the groundwork for further advancements. Future efforts could focus on improving performance by integrating whole-body and upper-body activity data and expanding testing to diverse real-world environments. Overall, this study advances wearable sensor-based activity recognition, supporting more effective ergonomic assessments and interventions to reduce musculoskeletal disorders across industries.

4 Quantifying Physical Exposures

4.1 Introduction

Accurately quantifying ergonomic exposures associated with MMH tasks is essential for physical demand analysis to protect workers' musculoskeletal health. Reliable assessments of these exposures are critical for developing effective interventions to mitigate WMSDs. Lifting, as a dynamic and highly variable activity, can be characterized by its duration, frequency, and magnitude (e.g., posture and load weight). As the frequency of lifting increases, physiological responses such as respiration rate and heart rate also rise, reflecting the growing physical demands on the body (Alferdaws and Ramadan 2020; Ghaleb et al. 2019). Awkward postures and heavy physical loads require sustained muscle force over extended periods, further contributing to cumulative fatigue and strain (Gallagher et al. 2002) . Each of these factors uniquely impacts the mechanical load on the lower back, underscoring the importance of comprehensive exposure assessments to better understand and reduce the risk of WMSDs (van Dieën et al. 2010; Hoozemans et al. 2008).

Several risk assessment methods, such as self-reports and observational approaches, have been developed to evaluate the risk of injury associated with manual lifting tasks (David 2005; Ramdan, Zulfikar, and Sahrijuita 2024). However, these subjective methods rely heavily on human judgment, which can reduce their validity and reliability. In addition to these subjective methods, various objective ergonomic risk assessment tools have been developed and are widely used to analyze physical exposures during lifting activities in the workplace (David 2005; Joshi and Deshpande 2019).

One of the most widely used tools for assessing manual lifting tasks is the Revised NIOSH Lifting Equation (RNLE). This tool evaluates the physical demands of two-handed manual lifting tasks and identifies conditions that may increase the risk of WMSDs (T. R. Waters, Putz-Anderson, and Garg 1994). The RNLE provides a quantitative framework for assessing lifting tasks by incorporating six critical parameters:

- Horizontal Location (H)
- Vertical Location (V)
- Vertical Travel Distance (D)
- Asymmetry Angle (A)
- Frequency (F)
- Coupling quality (C)

The Recommended Weight Limit (RWL) is calculated using these parameters, representing the maximum safe weight a worker can lift under specific conditions. The Lifting Index (LI) is then derived by comparing the actual weight of the load to the RWL. An LI value greater than 1 indicates a higher risk of injury.

Other ergonomic risk assessment methods for lifting include the American Conference of Governmental Industrial Hygienists (ACGIH) Lifting Threshold Limit Values (TLVs) and the Liberty Mutual “Snook” Lifting Tables (Russell et al. 2007), These tools also require the measurement of key parameters such as lifting frequency, horizontal location, and vertical location of the lift origin.

Accurately quantifying physical exposures is crucial for risk assessment and is typically carried out by experts observing workers during manual lifting tasks. Observers may count the lifting frequency manually and measure the vertical and horizontal locations using tools such as tape measures or laser devices. Nowadays, video analysis or wearable technologies are sometimes used for greater precision and reliability (Conforti et al. 2020; Lu et al. 2019; X. Wang et al. 2019; Xu et al. 2011). While video-based techniques provide a more reliable approach for identifying physical exposures, their performance can be affected by factors such as lighting conditions, self-occlusion, and environmental occlusions (MassirisFernández et al. 2020).

Inertial measurement units are capable of measuring position, velocity and acceleration, which are suitable for tracking the movement of workers in a long period. For example, Thomas et al. developed a machine learning framework that utilizes IMU-based kinematic data to detect lifting actions and classify their risk levels into four categories, achieving a balanced accuracy of 93% (Thomas et al. 2022). Donisi et al. developed a logistic regression model using data from a single IMU to classify lifts into two risk categories (risk and no risk) based on RNLE, achieving 82.8% accuracy (Donisi et al. 2022). However, many current studies prioritize categorical risk classification based on RNLE guidelines rather than directly quantifying physical exposures. This focus may limit their adaptability to scenarios with varied parameters (e.g., load weight, coupling quality), underscoring the need for ergonomic interventions capable of identifying and addressing high-risk exposures in a wider range of conditions. Barim et al. leveraged IMUs to measure lifting parameters, achieving errors of ~1 second for lifting duration, 33 cm for vertical distance, and 6.5 cm for horizontal distance when compared to a motion capture system (Barim et al. 2019).

Previous studies have largely analyzed lifting activities in isolation. In contrast, Phases I and II of this thesis leverage deep learning to identify lifting activities within complex work tasks, simulating real-world conditions. Building on these foundations, Chapter 4 introduces a novel approach to measure the physical exposures required for the Revised NIOSH Lifting Equation (RNLE), offering an automated, less intrusive, and highly valid method for ergonomic risk assessment of manual lifting.

The primary objective of this study is to develop a method for recognizing lifting durations within complex tasks using inertial measurement units (IMUs). This method processes the identified lifting durations to determine precise timestamps for the origin and destination of lifts. By doing so, it enables accurate and reliable quantification of key physical exposures, such as lifting frequency (F), horizontal location (H), and vertical location (V) at both the origin and destination of lifts. These measurements provide essential inputs for ergonomic risk assessment, particularly the RNLE, and physical demand analysis.

4.2 Methods

4.2.1 Participants and Devices

This laboratory-based study involved thirty participants and utilized a system of 17 inertial measurement units (IMUs). For detailed information, refer to Chapter 3.2.1.

4.2.2 Study Procedure

Participants first performed isolated functional activities, including lifting, pushing, pulling, carrying, and reaching above and below shoulder non-material handling (non-MMH) activities (e.g., walking or sitting with arms in a neutral position). These isolated activities were used to train a convolutional neural network (CNN) model to accurately recognize and classify movements. Participants also completed simulated work tasks that incorporated a variety of activities, including lifting. The trained CNN model was applied to these tasks to identify specific activities within 1-second time windows. MVTA served as the gold standard for accurately identifying the activities performed each second and was used to evaluate the CNN model's performance. This sequential classification provided a detailed, time-stamped record of task execution. Details refer to Chapter 3.

For the time windows identified as lifting by the CNN model, a hand velocity based method was employed to determine the precise origin (start) and destination (end) frames of each lifting event. This approach utilized changes in hand velocity to identify key moments corresponding to the beginning and end of lifting movements. The predicted frames were then compared to the ground truth frames, which were manually identified through detailed analysis of GoPro video recordings and Xsens motion-capture system recordings to ensure accuracy.

Once the lifting events were validated, the IMU data was processed to compute the horizontal and vertical hand positions associated with both the true and predicted origin and destination frames. These positions provided critical insights into the spatial characteristics of the lifting tasks and were integral to assessing the validity of the automated predictions. This workflow is illustrated in Figure 4-1, showcasing the integration of video analysis, IMU data processing, and model outputs to accurately quantify lifting-related physical exposures

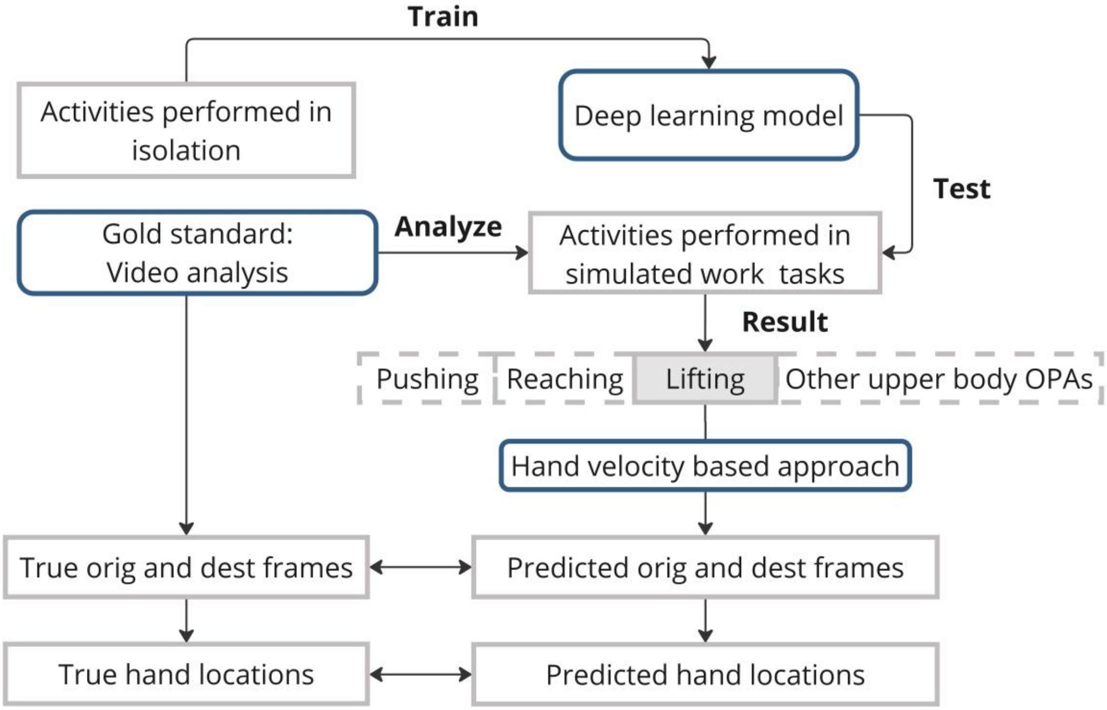

Figure 4-1 Study procedure for predicting lift origin and destination

4.2.3 Experimental Protocol

4.2.3.1 Lifting Performed in Isolation

As discussed in Chapter 3.2, activities were performed in isolation by each participant. For manual lifting, boxes were color-coded by weight (green for 2 kg, yellow for 5 kg, and red for 7 kg) and positioned at one of six locations: two horizontal positions (left or right) on one of three heights (floor, 76.2 cm, and 152.4 cm) (Figure 3-2). These six locations, labeled through A to F, were designed to simulate a range of common manual material handling (MMH) scenarios. On the floor, two markings (30 cm and 60 cm) indicated the horizontal hand positions where participants began each lift. While participants could step forward as needed, they were required to initiate each lift from the designated starting position.

The lifting parameters were based on the revised NIOSH lifting equation to represent common MMH tasks while minimizing injury risk. To further reduce injury risk, the heaviest weight (7 kg) was lifted only from the closer horizontal location. For each lift, participants began from a designated position and lifted a box of a specified weight from one shelf height to another, following a predefined routine sequence: C→B→D→A→C →D→A→B. This routine was repeated until each participant completed all combinations of shelf heights and weights. In total, each participant performed approximately 115 isolated, two-handed lifts.

Additionally, participants performed other isolated activities to supplement model training. For more details, refer to Chapter 3.2.3 and Table 3-2.

4.2.3.2 Lifting Performed in Simulated Work Tasks

The object sorting and carpet laying tasks were designed to incorporate various activities, including lifting, to simulate more complex work tasks (Figure 4-2b-d). Participants received verbal instructions prior to starting each task, along with occasional reminders, and physical demonstrations were provided upon request.

Object Sorting Task: Each participant sorted penny rolls and weights into two baskets. They began by lifting and carrying Basket A (2 kg) to place it on one of three available shelves (Figure 4-2b, c). Next, they returned to lift and carry Basket B (5 kg) to a different shelf. Finally, they lifted and carried a 7 kg box to place it on the remaining shelf. This task involved a total of six lifts (two of each weight), utilizing varied vertical hand positions (table, floor, and three shelf heights) and allowing participants flexibility in horizontal hand positioning for comfort (Table 4-1). Participants were instructed to use both hands when lifting the baskets and the box.

Carpet Laying Task: The participant lifted 12 carpets onto a cart in four separate lifts (4, 4, 2, and 2 carpets per lift). They then pushed and pulled the cart to a designated location, unloaded the carpets onto the floor in four lifts, and knelt to lay them in the specified area. Finally, the participant returned the cart to its original location by pushing and pulling. This task involved a total of eight lifts, with two vertical hand positions and varied horizontal hand locations (Table 4-1).

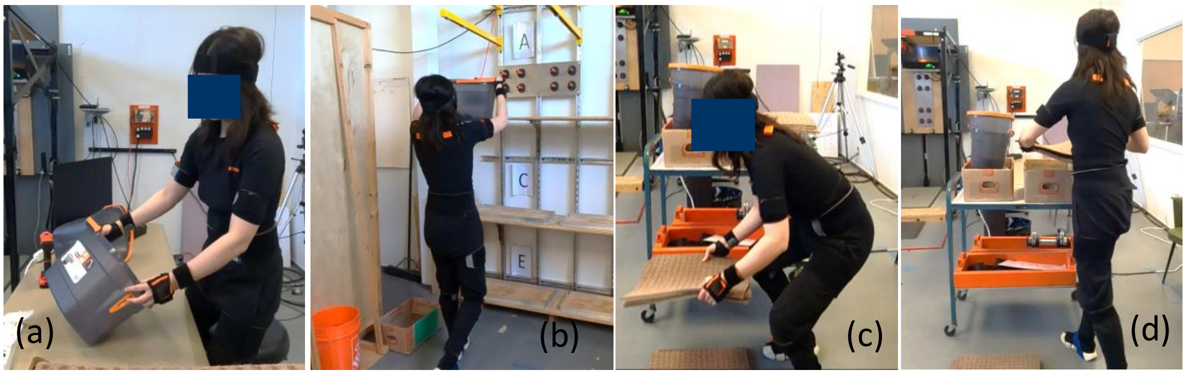

Figure 4-2 Lifting activities in simulated work tasks: (a) Participant lifting Basket A from the table to close to the body; (b) Participant lifting Basket A from close to the body to Shelf Height A; (c, d) Participant lifting four carpets from the ground to the cart.

Table 4-1 Lift details for object sorting and carpet laying tasks

	Lift #	From	To	Object	Load (kg)
Object sorting task	1	Table	Close to Body	Basket A	2
	2	Close to Body	Shelf Height A	Basket A	2
	3	Table	Close to Body	Basket B	5
	4	Close to Body	Shelf Height B	Basket B	5
	5	Table	Close to Body	Box C	7
	6	Close to Body	Shelf Height C	Box C	7
Carpet laying task	7	Floor	Cart	4 Carpets	4.25
	8	Floor	Cart	4 Carpets	4.25
	9	Floor	Cart	2 Carpets	2.13
	10	Floor	Cart	2 Carpets	2.13
	11	Cart	Floor	4 Carpets	4.25
	12	Cart	Floor	4 Carpets	4.25
	13	Cart	Floor	2 Carpets	2.13
	14	Cart	Floor	2 Carpets	2.13

4.2.4 Deep Learning Model

A ResNet-18 Convolutional Neural Network (CNN) model was used to recognize activities performed during simulated work tasks. Kinematic data from seventeen IMU sensors were processed into 1-second, image-like windows, each capturing movement features essential for activity classification.

The model was trained on data from isolated activity sessions, using a dataset split of 60% for training, 20% for validation, and 20% for testing. Training employed the Adam optimizer with a cross-entropy loss function and included regularization techniques, such as dropout layers, to mitigate overfitting. Following training, the model was applied to recognize activities within simulated work tasks. Model performance was evaluated by comparing it with Multimedia Video Task Analysis (MVTA), which served as the ground truth, providing accurate labels for each second of activity. Details refer to Chapter 3.2.5.

This approach enabled the model to generate a continuous timeline of task performance, identifying specific durations for each activity. By isolating segments identified as lifting, further analysis could be conducted on these time windows, including examining lift origin and destination, duration, and frequency.

4.2.5 Hand Velocity Approach

Following the identification of lifting segments in simulated work tasks by the CNN model, a hand-velocity-based approach was applied to analyze IMU data, specifically velocity and position, within these time windows to accurately determine the origin and destination frames for each lift. The velocity of each hand in 3D space (overall spatial velocity) and the average hand velocity were calculated and plotted for further analysis. This approach is based on the assumption that, when lifting an object at either the origin or destination, there is a distinct change in hand movement path, resulting in a low peak in hand velocity.

This approach does not examine instances when participants lifted the object close to the body to begin carrying or when they lifted it from the body after carrying it, as these scenarios do not necessarily involve a distinct change in hand movement path. Moreover, lifting close to the body generally poses a lower risk of injury than lifting away from the body, and is therefore outside the scope of this study. Consequently, each participant was expected to perform 14 lifts, with 22 origin and destination frames to be identified by this approach during the simulated tasks.

While the model is designed to classify reaching activities below shoulder height as 'Below Shoulder Non-MMH Movement,' an additional filtering step was applied to further exclude potential reaching periods. This refinement was necessary because the CNN model generates one prediction per second (across 60 frames), which means a segment predicted as lifting may still contain frames of reaching. To address this, a filter based on changes in hand location was applied, as the hand position shifts more distinctly once lifting begins, helping to isolate lifting movements from reaching activities.

After filtering, the average hand movement data were normalized using the 25th percentile (quantile 0.25) to ensure consistent data scaling across participants and tasks. The velocity curve was then smoothed to reduce noise, and negative peaks were identified as potential indicators of lifting movements. To refine peak selection further, a slope filter was applied with a set threshold for the velocity’s slope before and after each peak, isolating peaks more likely to represent actual lifting. Additionally, a maximum allowable velocity threshold was set to exclude any peaks above this threshold, based on the assumption that low velocity reflects changes in hand movement path at the start and end of a lift.

Further refinement involved excluding peaks where the difference between right and left-hand velocities exceeded the 60th percentile, as asymmetric hand velocities are less likely to represent two-handed lifting. The remaining peaks were sorted by their corresponding velocities, from smallest to largest. For periods identified as potential lifts, if the duration of the lifting curve was less than 240 frames (4 seconds), only the first two peaks were retained, as they were deemed most likely to represent the start and end of the lifting action. For longer periods, all remaining peaks were retained for analysis.

In cases where any remaining peaks occurred within 30 frames (0.5 seconds) of each other, they were averaged to yield a single representative peak, while retaining the rest. Finally, if no peaks were initially identified, the algorithm ran up to three additional loops, adding 30 frames with each iteration until at least one peak was found.

To evaluate the accuracy of the hand velocity approach in identifying lift origin and destination frames, video analysis was conducted using the combination of GoPro footage and Xsens-recorded video. This provided the true frames marking the start and end of each lift, which were then compared to the hand velocity approach results. Predictions were considered as correct if the differences fell within 30 frames (0.5 seconds).

4.2.6 Hand Locations

After identifying the origin and destination frames of the lift, the next step is to calculate the horizontal and vertical locations for further ergonomic risk assessment. According to the RNLE (Dawad et al. 2024; T. R. Waters, Putz-Anderson, and Garg 1994), the horizontal location (H) is defined as the distance from the midpoint of the line joining the inner ankle bones to a projected point on the floor directly beneath the midpoint of the hand grasp, which corresponds to the load center. In this study, foot-mounted IMUs positioned close to the ankles were used to approximate the ankle location for calculating the horizontal hand position.

The vertical location (V) is defined as the vertical height of the hands above the floor, measured from the floor to the midpoint between the hand grasps, as determined by the large middle knuckle. The z-axis height from the foot-mounted IMUs were utilized to estimate floor height. Although additional adjustments, such as shoe clearance, could be factored in for finer-grained analyses, these were not included in the current study. The H and V locations are essential in calculating the horizontal multiplier (HM) and vertical multiplier (VM), which are components for applying the RNLE to compute the RWL. Under ideal conditions, both HM and VM achieve their maximum value of 1.

The horizontal and vertical locations in this study were calculated as follows:

$$MP_{Ankles,\ xy} = (\frac{x_{RightFoot}+x_{LeftFoot}}{2}, \frac{y_{RightFoot}+y_{LeftFoot}}{2}) \tag{4-1}$$

$$MP_{Hands,\ xy} = (\frac{x_{RightFoot}+x_{LeftFoot}}{2}, \frac{y_{RightFoot}+y_{LeftFoot}}{2}) \tag{4-2}$$

$$H = \sqrt{\left(MP_{Hands,\ xy,x} - MP_{Ankles,\ xy,x}\right)^2 + \left(MP_{Hands,\ xy,y} - MP_{Ankles,\ xy,y}\right)^2} \tag{4-3}$$

$$V = \frac{z_{RightHand}+z_{LeftHand}}{2} - \frac{z_{RightFoot}+z_{LeftFoot}}{2} \tag{4-4}$$

where *MP* represents the midpoint.

Horizontal and vertical locations were calculated based on both the predicted origin and destination frames identified by the hand velocity approach and the true origin and destination frames marked through video analysis. The differences between the predicted and actual locations were then calculated to evaluate the performance of this approach.

4.3 Results

Thirty participants (18 females and 12 males) with a mean age of 28.3 years (SD = 8.2) participated in this laboratory study. None of the participants reported any recent injuries or chronic diseases.

4.3.1 Lifting Duration and Occurrence

Lifting in Isolation:

When activities were performed in isolation, data was collected over a 9-hour period. In the testing set, a total of 40 minutes and 11 seconds of lifting was performed, with the CNN model correctly identifying 99.1% of this lifting duration.

Lifting in Simulated Work Tasks:

In the simulated work tasks, participants performed a total of 21 minutes and 11 seconds of lifting. The CNN model accurately identified 81.6% of this lifting duration, equivalent to 17 minutes and 17 seconds. Additionally, 9.7% of the lifting duration was misclassified as below-shoulder non-MMH movements, while 4.7% was incorrectly recognized as carrying.

Lifting Counts in Simulated Work Tasks:

In the simulated tasks, a total of 412 lifts were performed and recorded using video analysis. The CNN model performed second-by-second activity recognition, with each continuous instance of lifting counted as a single lift for analysis. This process resulted in the identification of 454 lifts, representing 110.2% of the actual lifts performed.

Table 4-2 Summary of lifting duration, recognition accuracy, and counts in isolation and simulated work tasks

Condition	Total Duration	Recognized Duration	Accuracy	Total Counts	Identified Counts
In Isolation	40 min 11 sec	39 min 49 sec	99.10%	-	-
Work Tasks	21 min 11 sec	17 min 17 sec	81.60%	412	454

4.3.2 Origin and Destination Frames

Across the 412 lifts performed in the simulated work tasks, a total of 649 origin and destination frames were video identified, as lifts involving transitions to or from carrying activities were excluded from the scope of this analysis. The hand velocity approach accurately identified 508 of these frames, resulting in an overall accuracy of 78.3% across the thirty participants, defined by a frame difference threshold of 30 (0.5s). Seventeen participants achieved an accuracy exceeding 80%, while only one participant fell below 60% in correctly identifying origin and destination frames (Figure 4-3a). For all origin and destination frames, the mean frame difference between the predicted frames and the true frames identified via video analysis was 8.25, with a standard deviation of 7.27, as details illustrated in Figure 4-3b.

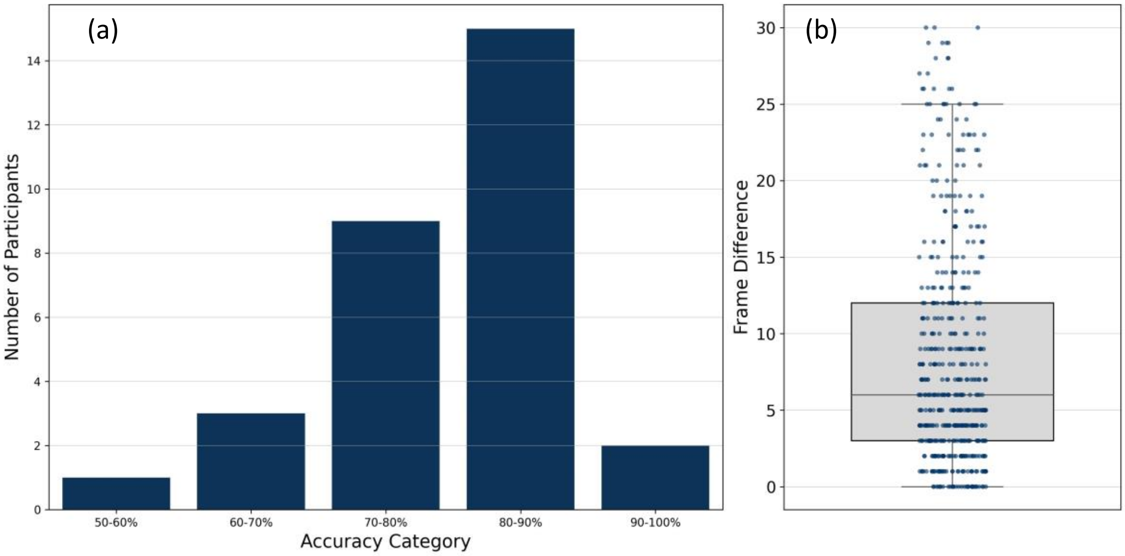

Figure 4-3 Performance of the hand velocity approach in predicting origin and destination frames of lifts: (a) Accuracy distribution for each participant in correctly identifying origin and destination frames; (b) Frame differences between predicted and actual frames for correctly identified origin and destination frames

4.3.3 Locations

Horizontal and vertical hand locations were calculated for the predicted and true origin and destination frames of each lift identified using the hand velocity approach. Discrepancies between predicted and true hand locations were quantified, with cases where the horizontal or vertical location difference exceeded 10 cm classified as outliers and excluded from further analysis (16 out of 508 identified origins/destinations, 3.1%). The distribution of the remaining discrepancies is illustrated in Figure 4-4.

Besides, a total of 7.5% of frames exhibited horizontal or vertical location differences within the range of 5–10 cm. The mean and standard deviation of the horizontal location discrepancies were 1.15 cm and 1.61 cm, respectively, while the mean and standard deviation of the vertical location discrepancies were 1.11 cm and 1.50 cm, respectively. Detailed distributions are also depicted in Figure 4-4.

A comparative visualization of the spatial distribution of horizontal and vertical locations based on the true and predicted origin and destination frames across the horizontal and vertical axes is shown in Figure 4-5. The analysis revealed that the spatial trends of locations observed from the predicted frames closely align with those derived from the true frames.

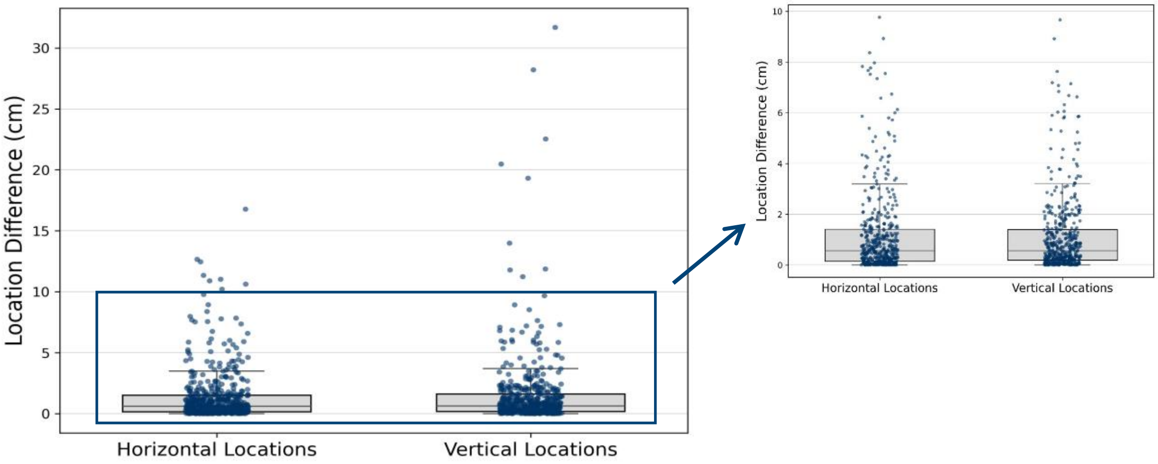

Figure 4-4 Horizontal and vertical location differences (cm) between predicted and true origin/destination frames

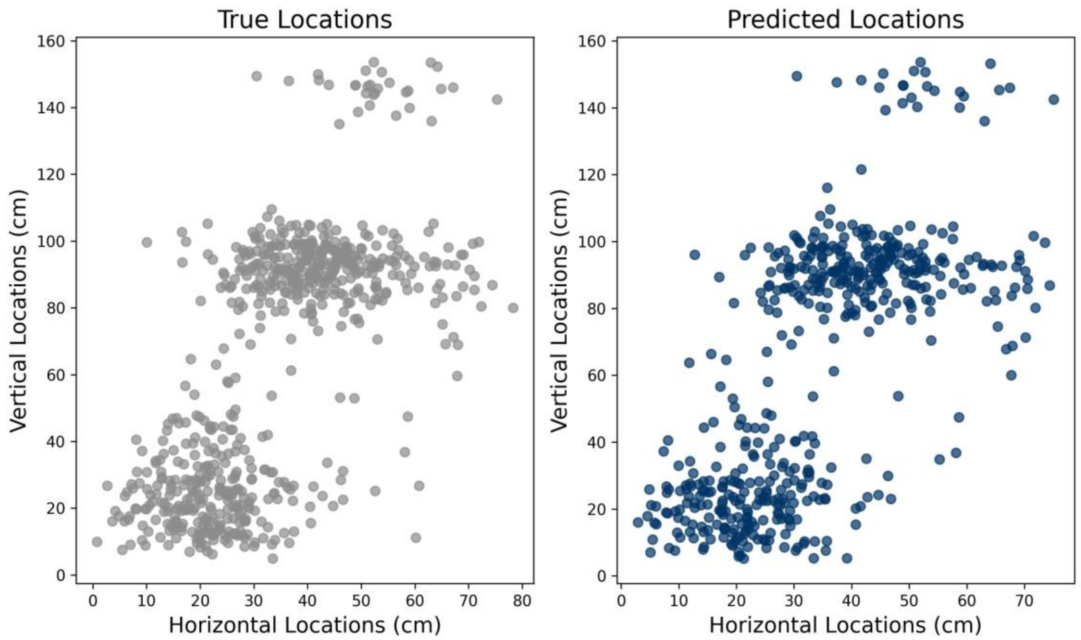

Figure 4-5 Comparison of hand locations calculated based on true and predicted origin/destination frames across horizontal and vertical axes.

4.4 Discussions

In this study, the integration of wearable devices, deep learning techniques, and the hand velocity approach demonstrated effective performance in identifying lifting activities. Specifically, the method correctly identified 81.6% of lifting durations and 110.2% of the actual lifting counts. The hand velocity approach was able to pinpoint 78.3% of the lift origin and destination frames within a 0.5-second margin, and 96.9% of the identified frames had hand positions within a 10 cm difference from the true frames. These results suggest minimal interference with ergonomic risk assessments, highlighting the effectiveness of this approach in accurately detecting two-handed lifts and providing reliable parameters for evaluating ergonomic risks.

This approach successfully recognized lifting activities for 99.1% of the duration when performed in isolation and 81.6% of the duration when performed as part of more complex, simulated work tasks (Table 4-2). However, the diverse ways in which lifts are performed—such as variations in locations, postures, and the items handled—pose ongoing challenges. Additionally, some lifting patterns closely resemble those of other activities, leading to the misclassification of 9.7% of lifting duration as below-shoulder non-MMH movements. Traditionally, activity duration has been collected using self-reports or through direct observer assessment (David 2005). However, self-reports can be biased by the worker's perception of exposure, with factors like severe low back pain potentially leading workers to overestimate the duration or frequency of physical loads (Viikari-Juntura et al. 1996). Observer-based methods often rely on broad categories (e.g., never, frequent, constant) to estimate activity duration, or, in some cases, record duration on an hourly scale, such as in the RNLE (short, moderate, and long duration). Consequently, the performance of this approach demonstrates clear advantages over traditional methods of recognizing lifting periods.

Additionally, this approach recorded 110.2% of the actual lifts performed, with overestimation commonly observed in carpet laying tasks, where participants were required to sort four carpets before lifting them from the ground or cart. The sorting process, which typically takes a few seconds, is recognized by the CNN model on a per-second basis. As a result, a single lift may be counted as two due to the sorting period, which is classified as below-shoulder non-MMH activity. Furthermore, when two lifts occur in rapid succession (within a 1-second interval), the model can only detect one consecutive lift occurrence. Accurate lift counts are crucial for calculating lift frequency (lifts/min) to apply RNLE (Dawad et al. 2024). While the slight overestimation observed in this study is unlikely to significantly impact the ergonomic risk, this limitation may become more pronounced in different settings or specific lift tasks, indicating the need for further refinement of the method for those contexts.

The hand-velocity approach was applied to identify the origin and destination frames of lifts, with the differences illustrated in Figure 4-6. A ±30-frame margin (equivalent to ±0.5 seconds) was used to evaluate the accuracy of frame identification. Correct identifications, defined as frame differences within this margin, accounted for 77% of all identified frames (Figure 4-3b). In a study by Barim et al., five IMUs and a lifting detection model were used to measure lift duration, reporting average accuracy differences of approximately 1 second (Barim et al. 2019). Specifically, the differences at the beginning of the lift ranged from 1.14 to 1.84 seconds, while differences at the end of the lift ranged from 1.52 to 2.20 seconds. By utilizing additional IMUs and applying the hand-velocity approach, this study achieves strong temporal alignment in a comprehensive task setting.

The incorrectly identified frames were primarily associated with periods when participants were sorting objects/carpets. Although the CNN model was designed to classify these periods as “below shoulder non-MMH activity” rather than lifting, some instances were still misclassified as lifting and included in the hand-velocity analysis. There are two potential reasons for this. First, the CNN model misclassified 12.8% of below-shoulder non-MMH activity as lifting. Second, the model made predictions on a 1-second basis, which could capture partial reaching movements. During reaching activity, changes in hand movement paths may have caused a low peak in hand velocity, triggering identification by the hand-velocity approach. To mitigate this, the study employed a filter based on changes in hand locations to distinguish lifting movements from reaching activity. However, challenges remain in fully isolating these movements. Despite some frames having relatively large differences from the true origin of the lift, the hand location—particularly the vertical location—tended to be similar to the true start point, suggesting that the impact on ergonomic risk assessment would be minor.

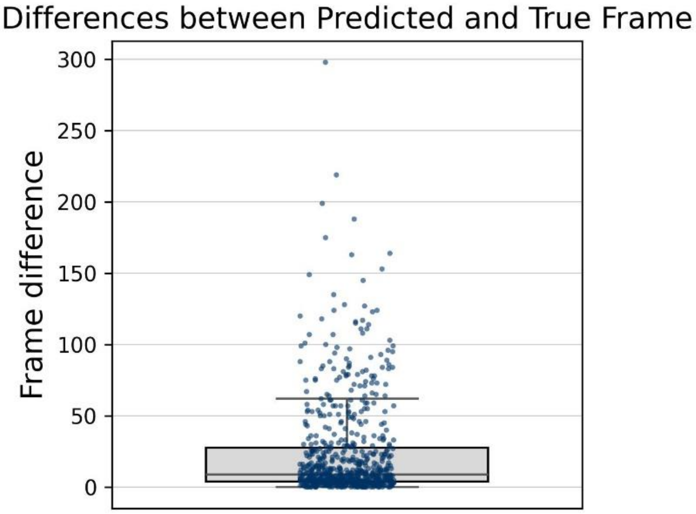

Figure 4-6 Difference between predicted and actual frames for the origins and destinations of lifts

Additionally, most participants (17 out of 30) achieved a frame identification accuracy exceeding 80%, with only one participant showing lower accuracy. This outlier can be attributed to the participant performing one-handed or asymmetric lifts multiple times when handling carpets. Participants were allowed to complete the carpet-laying task in their preferred manner. Since carpets are not rigid objects, it was natural for participants to lift one side first and secure the other side midway. This uneven movement often resulted in either the absence of a clear velocity peak for detection or filtering due to significant discrepancies between the movements of both hands. It is important to note that the most commonly used ergonomic risk assessment methods, such as RNLE, ACGIH TLVs, are not generally designed to account for one-handed lifting tasks. As such, one-handed lifting was not a focus of this study.

Among the correctly identified frames, 89.4% had both horizontal and vertical location differences within 5 cm, while 7.5% had at least one location difference between 5 and 10 cm. The impact of location differences on the HM and VM for predicted and true frames is summarized in Table 4-3. The true horizontal and vertical locations were selected based on the most commonly observed locations in this study (Figure 4-5). As shown, variations in VM are not affected by the true vertical location. When location differences are within 5 cm, or even up to 10 cm, their influence on VM remains minimal (< ±0.03), both in calculating the RWL and evaluating lifting risk. Location differences have a greater impact on HM, particularly when the horizontal location is small (closer to the body). However, when the difference is less than 5 cm, the influence on RWL remains limited. Notably, a margin of 5 cm represents a common and often unavoidable level of variation when experts use tape measurements to evaluate lifting activities. Some other lifting risk assessment tools use broader categories of location. For example, the ACGIH TLVs classify horizontal locations into three zones (close, mid, and far) and vertical locations into four general levels based on anatomical landmarks, such as shoulder, knuckle, and mid-shin height. Thus, the small location differences within 5 cm observed in this study are unlikely to have a significant impact on the accuracy of these assessments.

Table 4-3 Influence of location difference on RNLE parameters for predicted and true frames

True H (cm)	True V (cm)	Difference (cm)	HM difference †	VM differences ‡
25	20	5	(-0.16, 0)	(-0.02, +0.02)
		10	(-0.29, 0)	(-0.03, +0.03)
40	90	5	(-0.07, +0.09)	(-0.02, +0.02)
		10	(-0.13, +0.21)	(-0.03, +0.03)
50	150	5	(-0.05, +0.06)	(-0.02, +0.02)
		10	(-0.08, +0.13)	(-0.03, +0.03)

† Indicates the horizontal multiplier difference range.

‡ Indicates the vertical multiplier difference range.

This study utilized wearable technology, a deep learning framework, and a hand velocity-based approach to detect lifting activities and their durations, as well as to predict key exposure factors such as frequency and the horizontal and vertical locations at both the origin and destination of lifts. These outputs provide most of the essential exposure variables required for RNLE. Besides, the RNLE also requires the asymmetry angle and coupling factor to complete the risk assessment. While the IMU sensors is unlikely to estimate the coupling factor, calculating the asymmetry angle could be feasible. Incorporating this capability in future iterations could enable a more automated and comprehensive risk assessment, broadening the applicability of wearable technology for lifting-related risk evaluations.

Building on this, this study provides a novel capability to detect individual lifting activities and conduct ergonomic risk assessments for each lift performed. This approach differs from traditional methods, which typically observe workers over a 15-minute period and focus on the most common lifts or those with potentially higher risks. By enabling the automated measurement of every lift with minimal human intervention over prolonged durations, the methods used in this study may offer a more comprehensive understanding of the lifting activities that workers engage in. Such detailed, continuous data collection can capture the full range of exposure to ergonomic risks associated with manual lifting tasks.

The RNLE has been adapted and extended in various ways to better evaluate lifting tasks in diverse contexts. Examples include the Composite Lifting Index, Sequential Lifting Index, and Variable Lifting Index, among others (T. Waters et al. 2016; T. R. Waters, Putz-Anderson, and Garg 1994; T. R. Waters, Lu, and Occhipinti 2007). While these indices account for cumulative risk, they typically rely on task-based data, such as representative samples or aggregated categories, rather than tracking and assessing every single lift over extended durations. With the integration of wearable technologies and the approaches utilized in this study, there is a potential to develop a new lifting index capable of automatically capturing most individual lifts performed by a worker over hours or even an entire shift. This would enable a comprehensive risk assessment across all lifting activities performed by the worker. By building upon the methods demonstrated in this study, future advancements could significantly enhance both the precision and the practical application of risk assessments for manual lifting tasks.

4.5 Conclusions

This study integrated wearable devices, deep learning techniques, and a hand velocity-based approach to identify lifting activities and predict physical exposures for ergonomic risk assessment. The method demonstrated high accuracy in detecting lifting durations, counts, and hand positions, providing key exposure variables essential for the RNLE. Unlike traditional methods that focus on representative tasks, this approach has the potential to enable automated analysis of individual lifts over extended periods, offering a more detailed and comprehensive understanding of workers' manual lifting. Further improvements in accuracy and the inclusion of additional parameters, such as asymmetry, could enhance its capability for more comprehensive risk assessments. This framework holds significant promise for transforming ergonomic evaluations through precise and continuous risk assessments across diverse lifting tasks.

5 Conclusions

In Chapters 2 and 3 of this thesis, inertial measurement units and deep learning models were utilized to recognize occupational physical activities. The preliminary phase of these studies (Chapter 2) focused on using eight IMUs to recognize 15 distinct OPAs. While the model achieved a high accuracy of 95% for isolated activities, its performance declined significantly when applied to more complex tasks that combined multiple OPAs (n=9). In these scenarios, accuracy varied widely (0–95%) across activities, with an overall accuracy dropping to 22%. These findings indicate that while the model performed well in recognizing isolated activities, its reduced accuracy in complex tasks highlights the need for further development to enable reliable OPA recognition in real-world settings.

Building on these insights, Chapter 3 presents a more comprehensive study to address the challenges identified in the preliminary phase. This study utilized 17 IMUs and deep learning techniques to recognize 13 OPAs, categorized into seven whole-body and six upper-body activities, both in isolation and within three simulated work tasks designed to mimic real-world conditions. By addressing the influence of simultaneous activities, this study aimed to enhance model performance.

Thirty participants took part in the study, and the results demonstrated significant improvements. The whole-body activity recognition model achieved 99.1% accuracy for isolated activities and 89.0% for simulated tasks, while the upper-body activity recognition model achieved 98.2% accuracy in isolation and 84.8% in simulated tasks. Additionally, leave-group-out cross-validation confirmed the model's robustness and its potential for broader application across diverse populations. These findings suggest that the improved approach provides a reliable and valid method for quantifying OPAs, with substantial potential for practical application in occupational settings that involve complex task performance.

Building on the identification of OPAs, Chapter 4 focused on quantifying physical exposures, particularly for manual lifting tasks. Using the lifting activity periods identified by the deep learning model in Chapter 3, a hand velocity approach was introduced to predict lift origin and destination frames and calculate essential physical exposure parameters for ergonomic risk assessment.

This integrated approach demonstrated effective performance, capturing 81.6% of lifting periods and 110.2% of lifting counts. The hand velocity approach accurately identified 78.3% of lift origins and destinations, with the majority of frames closely aligning with their true positions. By providing essential exposure variables for ergonomic evaluations, this method shows the ability to enable automated analysis of individual lifts over extended periods. This capability offers a more detailed and comprehensive understanding of workers' manual lifting patterns and holds significant potential for transforming ergonomic risk assessments across diverse occupational settings.

This thesis advances the field of physical demand analysis and ergonomic evaluation by integrating wearable devices and deep learning techniques to recognize occupational physical activities and quantify physical exposures. Through innovative methodologies and rigorous evaluation, the research demonstrates the potential of these technologies to address the limitations of traditional approaches, such as reliance on manual observation and representative task analysis, which often lack reliability, consistency, and efficiency. For example, conventional methods typically involve experts observing manual material handling activities, such as lifting, for about 15 minutes and analyzing a limited sample of lifts—usually either common lifts or those deemed to have high-risk potential. This process often fails to capture the full scope of a worker's physical demands across an entire shift. By contrast, the approach developed in this research could enable a comprehensive risk assessment of all lifting activities performed by a worker, providing a more complete and accurate evaluation of occupational exposures.

The proposed methods demonstrate reliable recognition of OPAs and accurate measurement of key exposure parameters for manual lifting, providing practical applications to enhance workplace safety, reduce the risk of work-related musculoskeletal disorders, and improve ergonomic evaluations. By bridging the gap between controlled simplified settings and real-world complexities, this research establishes a solid foundation for advancing ergonomic assessment methodologies. It highlights the potential of wearable technology and deep learning to enable continuous and detailed monitoring of physical demands, paving the way for more tailored, comprehensive approaches to worker safety and health.

From a regulatory standpoint, this research enables companies and agencies, such as the Occupational Safety and Health Administration (OSHA), to adopt data-driven strategies to enhance compliance with safety standards. Wearable technology and automated analytics provide objective, quantifiable evidence of workplace risks, reducing reliance on subjective observations and streamlining audits. For companies, this approach transforms workplace safety management by enabling continuous risk assessments to proactively identify hazards, reduce injuries, and improve employee well-being. Automated monitoring also minimizes manual data collection, freeing resources for other priorities while demonstrating a strong commitment to safety and regulatory compliance.

The findings highlight the effectiveness of automated and scalable solutions in addressing challenges faced in real-world occupational settings. While further investigation is needed to fully implement this approach in field studies, we have already gained valuable experience using these devices to collect data from janitorial workers across various environments, including airports and shopping centers. Our observations suggest that these devices can effectively monitor workers' movements over extended periods without significant data drift during pilot data collection. Although additional research is required, we are confident that this approach has strong potential for widespread application in real-world scenarios.

Future efforts should focus on validating these methods through larger-scale field studies and refining the technology for enhanced usability and cost-effectiveness. Reducing the number of required sensors and integrating complementary technologies, such as video-based systems, could further improve performance while minimizing costs. Additionally, incorporating parameters like asymmetry angles and extending the approach to a broader range of MMH activities—such as carrying, pushing, and pulling—could significantly expand its applicability. Given the reliable performance of this approach in manual lifting tasks, it holds significant promise for broader ergonomic risk assessments.

These advancements could revolutionize how physical demands are analyzed, making ergonomic evaluations more adaptive, precise, and impactful across diverse occupational environments. Ultimately, this research demonstrates the transformative potential of integrating wearable technology and deep learning into workplace ergonomics, paving the way for safer, more efficient work environments and data-driven strategies for worker health and safety.

Bibliography

"2022 Workplace Safety Index." 2022. Liberty Mutual Business Insurance. *Liberty Mutual Business Insurance* (blog). 2022. https://business.libertymutual.com/insights/2022-workplace-safety-index/.

Agarwal, Shuchi, Craig Steinmaus, and Carisa Harris-Adamson. 2018. "Sit-Stand Workstations and Impact on Low Back Discomfort: A Systematic Review and Meta-Analysis." *Ergonomics* 61 (4): 538–52. https://doi.org/10.1080/00140139.2017.1402960.

Ahmad, Saman, and Mohammad Muzammil. 2023. "Revised NIOSH Lifting Equation: A Critical Evaluation." *International Journal of Occupational Safety and Ergonomics* 29 (1): 358–65. https://doi.org/10.1080/10803548.2022.2049123.

Ainsworth, Barbara E., Carl J. Caspersen, Charles E. Matthews, Louise C. Mâsse, Tom Baranowski, and Weimo Zhu. 2012. "Recommendations to Improve the Accuracy of Estimates of Physical Activity Derived From Self Report," January. https://doi.org/10.1123/jpah.9.s1.s76.

Alferdaws, Fares F., and Mohamed Z. Ramadan. 2020. "Effects of Lifting Method, Safety Shoe Type, and Lifting Frequency on Maximum Acceptable Weight of Lift, Physiological Responses, and Safety Shoes Discomfort Rating." *International Journal of Environmental Research and Public Health* 17 (9): 3012. https://doi.org/10.3390/ijerph17093012.

Antwi-Afari, Maxwell Fordjour, Heng Li, Yantao Yu, and Liulin Kong. 2018. "Wearable Insole Pressure System for Automated Detection and Classification of Awkward Working Postures in Construction Workers." *Automation in Construction* 96 (December):433–41. https://doi.org/10.1016/j.autcon.2018.10.004.

Baklouti, Souha, Abdelbadia Chaker, Taysir Rezgui, Anis Sahbani, Sami Bennour, and Med Amine Laribi. 2024. "A Novel IMU-Based System for Work-Related Musculoskeletal Disorders Risk Assessment." *Sensors* 24 (11): 3419. https://doi.org/10.3390/s24113419.

Barim, Menekse S., Ming-Lun Lu, Shuo Feng, Grant Hughes, Marie Hayden, and Dwight Werren. 2019. "Accuracy of An Algorithm Using Motion Data Of Five Wearable IMU Sensors For Estimating Lifting Duration And Lifting Risk Factors." *Proceedings of the Human Factors and Ergonomics Society Annual Meeting* 63 (1): 1105–11. https://doi.org/10.1177/1071181319631367.

Bastani, Kaveh, Sunwook Kim, Zhenyu Kong, Maury A. Nussbaum, and Wenzhen Huang. 2016. "Online Classification and Sensor Selection Optimization with Applications to Human Material Handling Tasks Using Wearable Sensing Technologies." *IEEE Transactions on Human-Machine Systems* 46 (4): 485–97. https://doi.org/10.1109/THMS.2016.2537747.

Bonde, Amelie, Shijia Pan, Mostafa Mirshekari, Carlos Ruiz, Hae Young Noh, and Pei Zhang. 2020. "OAC: Overlapping Office Activity Classification through IoT-

Sensed Structural Vibration." In *2020 IEEE/ACM Fifth International Conference on Internet-of-Things Design and Implementation (IoTDI)*, 216–22. https://doi.org/10.1109/IoTDI49375.2020.00028.

Boschman, Julitta S., Henk F. van der Molen, Judith K. Sluiter, and Monique H.W. Frings-Dresen. 2011. "Occupational Demands and Health Effects for Bricklayers and Construction Supervisors: A Systematic Review." *American Journal of Industrial Medicine* 54 (1): 55–77. https://doi.org/10.1002/ajim.20899.

Chen, Hao-ling, Keh-chung Lin, Rong-jiuan Liing, Ching-yi Wu, and Chia-ling Chen. 2015. "Kinematic Measures of Arm-Trunk Movements during Unilateral and Bilateral Reaching Predict Clinically Important Change in Perceived Arm Use in Daily Activities after Intensive Stroke Rehabilitation." *Journal of NeuroEngineering and Rehabilitation* 12 (1): 84. https://doi.org/10.1186/s12984-015-0075-8.

Chen, Jiayu, Jun Qiu, and Changbum Ahn. 2017. "Construction Worker's Awkward Posture Recognition through Supervised Motion Tensor Decomposition." *Automation in Construction* 77 (May):67–81. https://doi.org/10.1016/j.autcon.2017.01.020.

Chen, Kaixuan, Lina Yao, Dalin Zhang, Xianzhi Wang, Xiaojun Chang, and Feiping Nie. 2020. "A Semisupervised Recurrent Convolutional Attention Model for Human Activity Recognition." *IEEE Transactions on Neural Networks and Learning Systems* 31 (5): 1747–56. https://doi.org/10.1109/TNNLS.2019.2927224.

Coenen, Pieter, Vincent Gouttebarge, Aafje S. A. M. van der Burght, Jaap H. van Dieën, Monique H. W. Frings-Dresen, Allard J. van der Beek, and Alex Burdorf. 2014. "The Effect of Lifting during Work on Low Back Pain: A Health Impact Assessment Based on a Meta-Analysis." *Occupational and Environmental Medicine* 71 (12): 871–77. https://doi.org/10.1136/oemed-2014-102346.

Conforti, Ilaria, Ilaria Mileti, Zaccaria Del Prete, and Eduardo Palermo. 2020. "Measuring Biomechanical Risk in Lifting Load Tasks Through Wearable System and Machine-Learning Approach." *Sensors* 20 (6): 1557. https://doi.org/10.3390/s20061557.

Cuesta-Vargas, Antonio I, Alejandro Galán-Mercant, and Jonathan M Williams. 2010. "The Use of Inertial Sensors System for Human Motion Analysis." *Physical Therapy Reviews* 15 (6): 462–73. https://doi.org/10.1179/1743288X11Y.0000000006.

Daponte, Pasquale, Luca De Vito, and Carmine Sementa. 2013. "A Wireless-Based Home Rehabilitation System for Monitoring 3D Movements." In *2013 IEEE International Symposium on Medical Measurements and Applications (MeMeA)*, 282–87. https://doi.org/10.1109/MeMeA.2013.6549753.

David, G. C. 2005. "Ergonomic Methods for Assessing Exposure to Risk Factors for Work-Related Musculoskeletal Disorders." *Occupational Medicine* 55 (3): 190–99. https://doi.org/10.1093/occmed/kqi082.

Dawad, Noor Adillah, Siti Munira Yasin, Azlan Darus, Ahmad Taufik Jamil, and Nyi Nyi Naing. 2024. "Modification of the Revised National Institute for Occupational Safety and Health (NIOSH) Lifting Equation to Determine the

Individual Manual Lifting Risk in Malaysia's Manufacturing Industry." *Cureus* 16 (4): e57747. https://doi.org/10.7759/cureus.57747.

Dieën, Jaap H. van, Gert S. Faber, Romy C.C. Loos, P. Paul F.M. Kuijer, Idsart Kingma, Henk F. van der Molen, and Monique H.W. Frings-Dresen. 2010. "Validity of Estimates of Spinal Compression Forces Obtained from Worksite Measurements." *Ergonomics* 53 (6): 792–800. https://doi.org/10.1080/00140131003675091.

Donisi, Leandro, Giuseppe Cesarelli, Edda Capodaglio, Monica Panigazzi, Giovanni D'Addio, Mario Cesarelli, and Francesco Amato. 2022. "A Logistic Regression Model for Biomechanical Risk Classification in Lifting Tasks." *Diagnostics* 12 (11): 2624. https://doi.org/10.3390/diagnostics12112624.

"Ergonomics Program. | OSHA.Gov | Occupational Safety and Health Administration." 2001. 2001. https://www.osha.gov/laws-regs/federalregister/2001-04-23.

Escorcia, Víctor, María A. Dávila, Mani Golparvar-Fard, and Juan Carlos Niebles. 2012. "Automated Vision-Based Recognition of Construction Worker Actions for Building Interior Construction Operations Using RGBD Cameras," July, 879–88. https://doi.org/10.1061/9780784412329.089.

Gallagher, Sean. 2005. "Physical Limitations and Musculoskeletal Complaints Associated with Work in Unusual or Restricted Postures: A Literature Review." *Journal of Safety Research* 36 (1): 51–61. https://doi.org/10.1016/j.jsr.2004.12.001.

Gallagher, Sean, and William S. Marras. 2012. "Tolerance of the Lumbar Spine to Shear: A Review and Recommended Exposure Limits." *Clinical Biomechanics* 27 (10): 973–78. https://doi.org/10.1016/j.clinbiomech.2012.08.009.

Gallagher, Sean, William S. Marras, Kermit G. Davis, and Kimberly Kovacs. 2002. "Effects of Posture on Dynamic Back Loading during a Cable Lifting Task." *Ergonomics* 45 (5): 380–98. https://doi.org/10.1080/00140130210127639.

Ghaleb, Atef M., Mohamed Z. Ramadan, Ahmed Badwelan, and Khalid Saad Aljaloud. 2019. "Effect of Ambient Oxygen Content, Safety Shoe Type, and Lifting Frequency on Subject's MAWL and Physiological Responses." *International Journal of Environmental Research and Public Health* 16 (21): 4172. https://doi.org/10.3390/ijerph16214172.

Government of Canada, Canadian Centre for Occupational Health and Safety. 2024. "CCOHS: Return to Work - Job Demands Analysis." May 10, 2024. https://www.ccohs.ca/oshanswers/psychosocial/rtw/rtw_jobdemands.html.

GRANATA, KEVIN P., and WILLIAM S. MARRAS. 1999. "Relation between Spinal Load Factors and the High-Risk Probability of Occupational Low-Back Disorder." *Ergonomics* 42 (9): 1187–99. https://doi.org/10.1080/001401399185072.

Groh, Benjamin H, Thomas Kautz, Dominik Schuldhaus, and Bjoern M Eskofier. n.d. "IMU-Based Trick Classification in Skateboarding."

Hao Hu, Derek, Sinno Jialin Pan, Vincent Wenchen Zheng, Nathan Nan Liu, and Qiang Yang. 2008. "Real World Activity Recognition with Multiple Goals." In *Proceedings of the 10th International Conference on Ubiquitous Computing*, 30–39. Seoul Korea: ACM. https://doi.org/10.1145/1409635.1409640.

Harris-Adamson, Carisa, Ellen A. Eisen, Jay Kapellusch, Arun Garg, Kurt T. Hegmann, Matthew S. Thiese, Ann Marie Dale, et al. 2015. "Biomechanical Risk Factors for Carpal Tunnel Syndrome: A Pooled Study of 2474 Workers." *Occupational and Environmental Medicine* 72 (1): 33–41. https://doi.org/10.1136/oemed-2014-102378.

Harris-Adamson, Carisa, Alexis Mielke, Xu Xu, and Jia-Hua Lin. 2016. "Ergonomic Evaluation of Standard and Alternative Pallet Jack Handless." *International Journal of Industrial Ergonomics* 54 (July):113–19. https://doi.org/10.1016/j.ergon.2016.05.004.

He, Kaiming, Xiangyu Zhang, Shaoqing Ren, and Jian Sun. 2016. "Deep Residual Learning for Image Recognition." In , 770–78. https://openaccess.thecvf.com/content_cvpr_2016/html/He_Deep_Residual_Learning_CVPR_2016_paper.html.

Hoogendoorn, Wilhelmina E, Mireille NM van Poppel, Paulien M Bongers, Bart W Koes, and Lex M Bouter. 1999. "Physical Load during Work and Leisure Time as Risk Factors for Back Pain." *Scandinavian Journal of Work, Environment & Health* 25 (5): 387–403.

Hoozemans, Marco J.M., Idsart Kingma, Wiebe H.K. de Vries, and Jaap H. van Dieën. 2008. "Effect of Lifting Height and Load Mass on Low Back Loading." *Ergonomics* 51 (7): 1053–63. https://doi.org/10.1080/00140130801958642.

Humadi, Ahmed, Milad Nazarahari, Rafiq Ahmad, and Hossein Rouhani. 2021a. "In-Field Instrumented Ergonomic Risk Assessment: Inertial Measurement Units versus Kinect V2." *International Journal of Industrial Ergonomics* 84 (July):103147. https://doi.org/10.1016/j.ergon.2021.103147.

———. 2021b. "Instrumented Ergonomic Risk Assessment Using Wearable Inertial Measurement Units: Impact of Joint Angle Convention." *IEEE Access* 9:7293–7305. https://doi.org/10.1109/ACCESS.2020.3048645.

Huynh, Tâm, Mario Fritz, and Bernt Schiele. 2008. "Discovery of Activity Patterns Using Topic Models." In *Proceedings of the 10th International Conference on Ubiquitous Computing*, 10–19. UbiComp '08. New York, NY, USA: Association for Computing Machinery. https://doi.org/10.1145/1409635.1409638.

Ismail Fawaz, Hassan, Germain Forestier, Jonathan Weber, Lhassane Idoumghar, and Pierre-Alain Muller. 2019. "Deep Learning for Time Series Classification: A Review." *Data Mining and Knowledge Discovery* 33 (4): 917–63. https://doi.org/10.1007/s10618-019-00619-1.

Jancey, Jonine, Marian Tye, Sarah McGann, Krysten Blackford, and Andy H. Lee. 2014. "Application of the Occupational Sitting and Physical Activity Questionnaire (OSPAQ) to Office Based Workers." *BMC Public Health* 14 (1): 762. https://doi.org/10.1186/1471-2458-14-762.

Joshi, Mangesh, and Vishwas Deshpande. 2019. "A Systematic Review of Comparative Studies on Ergonomic Assessment Techniques." *International Journal of Industrial Ergonomics* 74 (November):102865. https://doi.org/10.1016/j.ergon.2019.102865.

Kelsey, Jennifer L., Penny B. Githens, Augustus A. White III, Theodore R. Holford, Stephen D. Walter, Theresa O'Connor, Adrian M. Ostfeld, Ulrich Weil, Wayne

O. Southwick, and John A. Calogero. 1984. “An Epidemiologic Study of Lifting and Twisting on the Job and Risk for Acute Prolapsed Lumbar Intervertebral Disc.” *Journal of Orthopaedic Research* 2 (1): 61–66. https://doi.org/10.1002/jor.1100020110.

Khosrowpour, Ardalan, Juan Carlos Niebles, and Mani Golparvar-Fard. 2014. “Vision-Based Workface Assessment Using Depth Images for Activity Analysis of Interior Construction Operations.” *Automation in Construction* 48 (December):74–87. https://doi.org/10.1016/j.autcon.2014.08.003.

Kim, Sunwook, and Maury A. Nussbaum. 2013. “Performance Evaluation of a Wearable Inertial Motion Capture System for Capturing Physical Exposures during Manual Material Handling Tasks.” *Ergonomics* 56 (2): 314–26. https://doi.org/10.1080/00140139.2012.742932.

Lin, Po-Chieh, Yu-Jung Chen, Wei-Shin Chen, and Yun-Ju Lee. 2022. “Automatic Real-Time Occupational Posture Evaluation and Select Corresponding Ergonomic Assessments.” *Scientific Reports* 12 (1): 2139. https://doi.org/10.1038/s41598-022-05812-9.

Lu, Ming-Lun, Shuo Feng, Grant Hughes, Menekse S. Barim, Marie Hayden, and Dwight Werren. 2019. “Development of an Algorithm for Automatically Assessing Lifting Risk Factors Using Inertial Measurement Units.” *Proceedings of the Human Factors and Ergonomics Society Annual Meeting* 63 (1): 1334–38. https://doi.org/10.1177/1071181319631252.

Lu, Ming-Lun, Thomas R. Waters, Edward Krieg, and Dwight Werren. 2014. “Efficacy of the Revised NIOSH Lifting Equation to Predict Risk of Low-Back Pain Associated With Manual Lifting: A One-Year Prospective Study.” *Human Factors* 56 (1): 73–85. https://doi.org/10.1177/0018720813513608.

Mäkela, Satu-Marja, Arttu Lämsä, Janne S. Keränen, Jussi Liikka, Jussi Ronkainen, Johannes Peltola, Juha Häikiö, Sari Järvinen, and Miguel Bordallo López. 2022. “Introducing VTT-ConIot: A Realistic Dataset for Activity Recognition of Construction Workers Using IMU Devices.” *Sustainability* 14 (1): 220. https://doi.org/10.3390/su14010220.

Marras, W. S. 2000. “Occupational Low Back Disorder Causation and Control.” *Ergonomics* 43 (7): 880–902. https://doi.org/10.1080/001401300409080.

MassirisFernández, Manlio, J. Álvaro Fernández, Juan M. Bajo, and Claudio A. Delrieux. 2020. “Ergonomic Risk Assessment Based on Computer Vision and Machine Learning.” *Computers & Industrial Engineering* 149 (November):106816. https://doi.org/10.1016/j.cie.2020.106816.

Melanson Jr., Edward L., Patty S. Freedson, and Steve Blair. 1996. “Physical Activity Assessment: A Review of Methods.” *Critical Reviews in Food Science and Nutrition* 36 (5): 385–96. https://doi.org/10.1080/10408399609527732.

Mo, Lingfei, Fan Li, Yanjia Zhu, and Anjie Huang. 2016. “Human Physical Activity Recognition Based on Computer Vision with Deep Learning Model.” In *2016 IEEE International Instrumentation and Measurement Technology Conference Proceedings*, 1–6. https://doi.org/10.1109/I2MTC.2016.7520541.

Mokhlespour Esfahani, Mohammad Iman, Maury A. Nussbaum, and Zhenyu (James) Kong. 2019. “Using a Smart Textile System for Classifying Occupational Manual Material Handling Tasks: Evidence from Lab-Based Simulations.”

Ergonomics 62 (6): 823–33. https://doi.org/10.1080/00140139.2019.1578419.

Nematallah, Heba, and Sreeraman Rajan. 2024. “Adaptive Hierarchical Classification for Human Activity Recognition Using Inertial Measurement Unit (IMU) Time-Series Data.” *IEEE Access* 12:52127–49. https://doi.org/10.1109/ACCESS.2024.3386351.

Odebiyi, Daniel O., Udoka Arinze Chris Okafor, Daniel O. Odebiyi, and Udoka Arinze Chris Okafor. 2023. “Musculoskeletal Disorders, Workplace Ergonomics and Injury Prevention.” In *Ergonomics - New Insights*. IntechOpen. https://doi.org/10.5772/intechopen.106031.

Okita, Tsuyoshi, and Sozo Inoue. 2017. “Recognition of Multiple Overlapping Activities Using Compositional CNN-LSTM Model.” In *Proceedings of the 2017 ACM International Joint Conference on Pervasive and Ubiquitous Computing and Proceedings of the 2017 ACM International Symposium on Wearable Computers*, 165–68. Maui Hawaii: ACM. https://doi.org/10.1145/3123024.3123095.

Olds, Tim S., Sjaan R. Gomersall, Spencer T. Olds, and Kate Ridley. 2019. “A Source of Systematic Bias in Self-Reported Physical Activity: The Cutpoint Bias Hypothesis.” *Journal of Science and Medicine in Sport* 22 (8): 924–28. https://doi.org/10.1016/j.jsams.2019.03.006.

“Physical Demands.” 2015. Bureau of Labor Statistics. 2015. https://www.bls.gov/ors/factsheet/physical-072015.htm.

Potvin, Jim R., Vincent M. Ciriello, Stover H. Snook, Wayne S. Maynard, and George E. Brogmus. 2021. “The Liberty Mutual Manual Materials Handling (LM-MMH) Equations.” *Ergonomics* 64 (8): 955–70. https://doi.org/10.1080/00140139.2021.1891297.

Ramdan, Muhamad, Iwan Zulfikar, and Sahrijuita Sahrijuita. 2024. “Manual Material Handling Analysisi Of Workers Lifting Goods Using The Rappid Upper Limb Assessment (Rula) Method At Pt Intipratama Global Service.” *Journal of Industrial System Engineering and Management* 3 (1): 1–7. https://doi.org/10.56882/jisem.v3i1.26.

Rodrigues, Patrick B., Yijing Xiao, Yoko E. Fukumura, Mohamad Awada, Ashrant Aryal, Burcin Becerik-Gerber, Gale Lucas, and Shawn C. Roll. 2022. “Ergonomic Assessment of Office Worker Postures Using 3D Automated Joint Angle Assessment.” *Advanced Engineering Informatics* 52 (April):101596. https://doi.org/10.1016/j.aei.2022.101596.

Russell, Steven J., Lori Winnemuller, Janice E. Camp, and Peter W. Johnson. 2007. “Comparing the Results of Five Lifting Analysis Tools.” *Applied Ergonomics* 38 (1): 91–97. https://doi.org/10.1016/j.apergo.2005.12.006.

Sangari, Arash, and William Sethares. 2016. “Convergence Analysis of Two Loss Functions in Soft-Max Regression.” *IEEE Transactions on Signal Processing* 64 (5): 1280–88. https://doi.org/10.1109/TSP.2015.2504348.

Schall, Mark C., Nathan B. Fethke, and Howard Chen. 2016. “Working Postures and Physical Activity among Registered Nurses.” *Applied Ergonomics* 54 (May):243–50. https://doi.org/10.1016/j.apergo.2016.01.008.

Song, Jiahong, and Xingda Qu. 2014a. "Age-Related Biomechanical Differences during Asymmetric Lifting." *International Journal of Industrial Ergonomics* 44 (5): 629–35. https://doi.org/10.1016/j.ergon.2014.06.008.

———. 2014b. "Effects of Age and Its Interaction with Task Parameters on Lifting Biomechanics." *Ergonomics* 57 (5): 653–68. https://doi.org/10.1080/00140139.2014.897376.

Steeves, Jeremy A., Catrine Tudor-Locke, Rachel A. Murphy, George A. King, Eugene C. Fitzhugh, David R. Bassett, Dane Van Domelen, John M. Schuna, and Tamara B. Harris. 2018. "Daily Physical Activity by Occupational Classification in US Adults: NHANES 2005–2006," December. https://doi.org/10.1123/jpah.2017-0465.

Strine, Tara W., and Jennifer M. Hootman. 2007. "US National Prevalence and Correlates of Low Back and Neck Pain among Adults." *Arthritis Care & Research* 57 (4): 656–65. https://doi.org/10.1002/art.22684.

Takala, Esa-Pekka, Irmeli Pehkonen, Mikael Forsman, Gert-Åke Hansson, Svend Erik Mathiassen, W Patrick Neumann, Gisela Sjøgaard, Kaj Bo Veiersted, Rolf H Westgaard, and Jørgen Winkel. 2010. "Systematic Evaluation of Observational Methods Assessing Biomechanical Exposures at Work." *Scandinavian Journal of Work, Environment & Health* 36 (1): 3–24.

Tammana, Aditya, Cody McKay, Stephen M. Cain, Steven P. Davidson, Rachel V. Vitali, Lauro Ojeda, Leia Stirling, and Noel C. Perkins. 2018. "Load-Embedded Inertial Measurement Unit Reveals Lifting Performance." *Applied Ergonomics* 70 (July):68–76. https://doi.org/10.1016/j.apergo.2018.01.014.

Tessendorf, Bernd, Franz Gravenhorst, Bert Arnrich, and Gerhard Tröster. 2011. "An IMU-Based Sensor Network to Continuously Monitor Rowing Technique on the Water." In *2011 Seventh International Conference on Intelligent Sensors, Sensor Networks and Information Processing*, 253–58. https://doi.org/10.1109/ISSNIP.2011.6146535.

"The ADA: Your Responsibilities as an Employer." n.d. US EEOC. Accessed October 10, 2024. https://www.eeoc.gov/publications/ada-your-responsibilities-employer.

Thiese, Matthew. 2013. "Important Differences in Accelerometer Cut Points for Quantifying Physical Activity in a Nested Occupational Cohort." *Journal of Exercise, Sports & Orthopedics* 1 (January). https://doi.org/10.15226/2374-6904/1/1/00102.

Thomas, Brennan, Ming-Lun Lu, Rashmi Jha, and Joseph Bertrand. 2022. "Machine Learning for Detection and Risk Assessment of Lifting Action." *IEEE Transactions on Human-Machine Systems* 52 (6): 1196–1204. https://doi.org/10.1109/THMS.2022.3212666.

Viikari-Juntura, Eira, Sirpa Rauas, Rami Martikainen, Eeva Kuosma, Hilkka Riihimäki, Esa-Pekka Takala, and Kari Saarenmaa. 1996. "Validity of Self-Reported Physical Work Load in Epidemiologic Studies on Musculoskeletal Disorders." *Scandinavian Journal of Work, Environment & Health* 22 (4): 251–59.

Villalobos, Adolfo, and Alejandro Mac Cawley. 2022. "Prediction of Slaughterhouse Workers' RULA Scores and Knife Edge Using Low-Cost Inertial Measurement

Sensor Units and Machine Learning Algorithms." *Applied Ergonomics* 98 (January):103556. https://doi.org/10.1016/j.apergo.2021.103556.

"Visual Overview for Physical Demands." n.d. Bureau of Labor Statistics. Accessed September 22, 2024. https://www.bls.gov/ors/factsheet/visual-overview-of-physical-demands.htm.

Wang, Mengcheng, Chuan Zhao, Alan Barr, Suihuai Yu, Jay Kapellusch, and Carisa Harris Adamson. 2020. "Hand Posture and Force Estimation Using Surface Electromyography and an Artificial Neural Network." *Proceedings of the Human Factors and Ergonomics Society Annual Meeting* 64 (1): 1247–48. https://doi.org/10.1177/1071181320641296.

Wang, Qi, Liesbet De Baets, Annick Timmermans, Wei Chen, Luca Giacolini, Thomas Matheve, and Panos Markopoulos. 2017. "Motor Control Training for the Shoulder with Smart Garments." *Sensors (Basel, Switzerland)* 17 (7): 1687. https://doi.org/10.3390/s17071687.

Wang, Xuan, Yu Hen Hu, Ming-Lun Lu, and Robert G. Radwin. 2019. "The Accuracy of a 2D Video-Based Lifting Monitor." *Ergonomics* 62 (8): 1043–54. https://doi.org/10.1080/00140139.2019.1618500.

Waters, T. R., M.-L. Lu, and E. Occhipinti. 2007. "New Procedure for Assessing Sequential Manual Lifting Jobs Using the Revised NIOSH Lifting Equation." *Ergonomics* 50 (11): 1761–70. https://doi.org/10.1080/00140130701674364.

Waters, Thomas, Enrico Occhipinti, Daniela Colombini, Enrique Alvarez-Casado, and Robert Fox. 2016. "Variable Lifting Index (VLI): A New Method for Evaluating Variable Lifting Tasks." *Human Factors* 58 (5): 695–711. https://doi.org/10.1177/0018720815612256.

Waters, T.R., Vern Putz-Anderson, and Arun Garg. 1994. "Applications Manual for the Revised NIOSH Lifting Equation," January. https://stacks.cdc.gov/view/cdc/5434.

"Work-Related Musculoskeletal Disorders & Ergonomics | Workplace Health Strategies by Condition | Workplace Health Promotion | CDC." 2021. May 12, 2021. https://www.cdc.gov/workplacehealthpromotion/health-strategies/musculoskeletal-disorders/index.html.

Xinming, Li, Gordon Fan, Abdullah Abudan, Majd Sukkarieh, Mustafa Gül, Marwan El-Rich, Mohamed Al-Hussein, and Ndukeabasi Inyang. 2015. "Ergonomics and Physical Demand Analysis in a Construction Manufacturing Facility." June 2015. https://doi.org/10.14288/1.0076405.

Xu, Xu, Chien-chi Chang, Gert S. Faber, Idsart Kingma, and Jack T. Dennerlein. 2011. "The Validity and Interrater Reliability of Video-Based Posture Observation During Asymmetric Lifting Tasks." *Human Factors* 53 (4): 371–82. https://doi.org/10.1177/0018720811410976.

Yan, Xuzhong, Heng Li, Chen Wang, JoonOh Seo, Hong Zhang, and Hongwei Wang. 2017. "Development of Ergonomic Posture Recognition Technique Based on 2D Ordinary Camera for Construction Hazard Prevention through View-Invariant Features in 2D Skeleton Motion." *Advanced Engineering Informatics* 34 (October):152–63. https://doi.org/10.1016/j.aei.2017.11.001.

Yan, Yishu, Hao Fan, Yibin Li, Elias Hoeglinger, Alexander Wiesinger, Alan Barr, Grace D. O'Connell, and Carisa Harris-Adamson. 2021. "Applying Wearable Technology and a Deep Learning Model to Predict Occupational Physical Activities." *Applied Sciences* 11 (20): 9636. https://doi.org/10.3390/app11209636.

Yang, Peicheng, Lei Xie, Chuyu Wang, and Sanglu Lu. 2019. "IMU-Kinect: A Motion Sensor-Based Gait Monitoring System for Intelligent Healthcare." In *Adjunct Proceedings of the 2019 ACM International Joint Conference on Pervasive and Ubiquitous Computing and Proceedings of the 2019 ACM International Symposium on Wearable Computers*, 350–53. UbiComp/ISWC '19 Adjunct. New York, NY, USA: Association for Computing Machinery. https://doi.org/10.1145/3341162.3343766.

Yeh, Shih Ching, Shun Min Chang, Wu Yuin Hwang, Wen Kang Liu, and Tzu Chuan Huang. 2013. "Virtual Reality Applications IMU Wireless Sensors in the Lower Limbs Rehabilitation Training." *Applied Mechanics and Materials* 278–280:1889–92. https://doi.org/10.4028/www.scientific.net/AMM.278-280.1889.

Yen, T.Y., and R.G. Radwin. 1995. "A Video-Based System for Acquiring Biomechanical Data Synchronized with Arbitrary Events and Activities." *IEEE Transactions on Biomedical Engineering* 42 (9): 944–48. https://doi.org/10.1109/10.412663.

Zhang, Hong, Xuzhong Yan, and Heng Li. 2018. "Ergonomic Posture Recognition Using 3D View-Invariant Features from Single Ordinary Camera." *Automation in Construction* 94 (October):1–10. https://doi.org/10.1016/j.autcon.2018.05.033.